

Climate Change Impact on the Hydropower Potential in Agder County

Case study: Tovdal Catchment Using an Educational Version of HBV

Hanna Andersen

SUPERVISOR

Joao Leal

University of Agder, 2023
Faculty of Engineering and Science
Department of Engineering and Sciences

Mandatory Declaration

1.	I/We hereby declare that my/our report is my/our work and that I/We have not used any other sources or have received any other help than mentioned in the report	<input checked="" type="checkbox"/> YES
2.	I/we further declare that this report:: <ul style="list-style-type: none"> • has not been used for another exam at another department/university college in Norway or abroad. • does not refer to the work of others without it being stated. • does not refer to own previous work without it being stated. • have all the references given in the literature list. • is not a copy, duplicate or copy of another's work or manuscript. 	<input checked="" type="checkbox"/> YES
3.	I/we am/are aware that violation of the above is regarded as cheating and may result in cancellation of exams and exclusion from universities and colleges in Norway, see Universitets- og høyskoleloven §§4-7 og 4-8 og Forskrift om eksamen §§ 31.	<input checked="" type="checkbox"/> YES
4.	I/we am/are aware that all submitted reports may be checked for plagiarism.	<input checked="" type="checkbox"/> YES
5.	I/we am/are aware that the University of Agder will deal with all cases where there is suspicion of cheating according to the university's guidelines for dealing with cases of cheating.	<input checked="" type="checkbox"/> YES
6.	I/we have incorporated the rules and guidelines in the use of sources and references on the library's web pages.	<input checked="" type="checkbox"/> YES

Publishing Agreement

Authorization for electronic publishing of the report.	
I hereby give the University of Agder a free right to make the task available for electronic publishing:	<input checked="" type="checkbox"/> YES
Is the report confidential?	<input checked="" type="checkbox"/> NO
Is the task except for public disclosure?	<input checked="" type="checkbox"/> NO

Acknowledgements

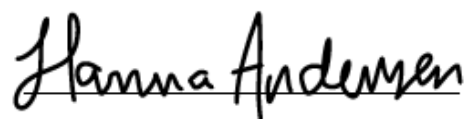
This master's thesis marks the final chapter of my academic journey, which included a one-year study in business economics from BI Norwegian Business School, a bachelor's degree in Electrical Engineering from the Norwegian University of Science and Technology and a master's degree in Renewable Energy from the University of Agder.

I started working on this master's thesis in January 2023, and after several months of effort, I successfully delivered the completed thesis in May 2023, corresponding to 30 study credits. The target audience for this thesis includes those with similar background knowledge as mine, those with an interest in hydrological modeling and those who share a curiosity in this specific field of study. I have managed to complete the project task and answer the research question of the thesis. I deliver this thesis with pride, confident in its contribution to the knowledge in the field and its potential impact on future research and understanding.

I would like to express my sincere gratitude to my supervisor Joao Leal, for his guidance, support, engagement with the topic and valuable advice throughout the semester. I am also deeply grateful for his assistance with Python programming, which has been crucial in the development of this thesis.

The biggest acknowledgment I want to dedicate to my father and grandfather, Erik Andersen and Gisle Erik Andersen, for their unwavering help and support throughout my academic journey. Without their help, I would not have been able to reach this point in my life.

I would also like to thank my family and friends for their support, encouragement and patience during the process of this thesis. Special thanks to Per Simen for his mental and technical support. His support helped me stay motivated and focused on completing this thesis.

A handwritten signature in black ink that reads "Hanna Andersen". The signature is written in a cursive, flowing style with a horizontal line underneath the name.

Grimstad, May 21, 2023

Abstract

Climate change poses significant uncertainties for the future of hydropower, both in terms of challenges and opportunities. This study uses an educational version of the HBV model to investigate climate change impact on the hydropower potential in Agder County over the next century. The results show that the model tends to overestimate the observed values, but results in a Nash-Sutcliffe efficiency of 73.4% for calibration and 77.7% for validation with a correlation of 89.0%. This indicates that the model's simplicity does not surpass its accuracy.

For annual discharge the study found that the RCP4.5 scenario predicted a 9% increase close to 2100. The RCP8.5 scenario projected a more significant increase, starting around 2040 and reaching a projection of 18% increase. Analysis of monthly discharge patterns revealed significant changes. There is a significant increase in the winter (November to April) for RCP4.5 and RCP8.5. The summer months (May to October) will have reduced discharge for both scenarios. RCP8.5 will have a more significant change than RCP4.5 in all months. The discrepancies between mid- and late-century were particularly pronounced from January to April, indicating a substantial increase in discharge over the century. This suggests a shift towards warmer and wetter winters in Agder County, leading to reduced snow accumulation.

The observed trends in future discharge patterns underline the challenges and opportunities associated with hydropower production in the face of climate change. During periods of reduced discharge, it is crucial for Agder County to have sufficient water stored in reservoirs to meet the power demand. The increasing discharge during winter can also present opportunities for hydropower production. By optimizing existing power plants, consider expansions of waterways and aggregates, as well as increased generator performance, it will be achieved increased production and better utilization of the increasing winter discharge.

Sammendrag

Klimaendringene medfører betydelig usikkerhet for fremtiden til vannkraft, både når det gjelder utfordringer og muligheter. Denne studien undersøker klimaendringenes innvirkning på vannkraftpotensialet i Agder fylke i løpet av det neste århundret ved hjelp av en versjon av HBV modellen ment for utdanningsformål. Resultatene viser at modellen har en tendens til å overestimere de observerte verdiene, men resulterer i en Nash-Sutcliffe effektivitet på 73,4% for kalibrering og 77,7% for validering med en korrelasjon på 89,0%. Dette indikerer at modellens forenklinger ikke går på bekostning av nøyaktigheten.

For årlig vannføring viser resultatene at RCP4.5-scenariet vil ha en økning på 9% mot slutten av århundret. RCP8.5-scenariet anslår en mer betydelig økning, som starter rundt 2040 og når 18% rundt 2100. Resultatene for månedlig vannføring viste større endringer. Det vil bli en betydelig økning i vintermånedene (november til april) for både RCP4.5 og RCP8.5. Sommermånedene (mai til oktober) vil ha redusert vannføring for begge scenariene. RCP8.5 vil ha en mer betydelig endring enn RCP4.5 i alle måneder. Avvikene mellom midten og sent i århundret er betydelige fra januar til april, noe som indikerer en betydelig økning i vannføring gjennom århundret. Dette tyder på at det blir varmere og våtere vintre i Agder fylke, med mindre snømengder.

De observerte trendene i fremtidig vannføring understreker utfordringene og mulighetene knyttet til vannkraftproduksjon i møte med klimaendringene. I tider med redusert vannføring er det avgjørende for Agder fylke å ha lagret nok vann i magasinene for å møte etterspørselen etter kraft. Den økende vannføringen på vinteren kan også åpne opp for muligheter innen vannkraftproduksjon. Ved å optimalisere driften av eksisterende kraftverk, vurdere utvidelser av vannvei, aggregat, samt økt generatorytelse, vil det oppnås økt produksjon og bedre utnyttelse av den økende vintervannføringen.

Contents

Acknowledgements	iii
Abstract	v
Sammendrag	vii
List of Figures	xii
List of Tables	xiii
Abbreviations	xvii
Nomenclature	xviii
1 Introduction	1
1.1 Research Question	4
1.2 Structure	4
2 Theory	5
2.1 Potential Hydropower	5
2.2 Thiessen Polygon Method	6
2.3 Hydrological Models	7
2.3.1 Empirical Models	7
2.3.2 Conceptual Models	8
2.3.3 Physically Based Models	8
2.4 Representative Concentration Pathways	9
3 Previous Studies	11
3.1 Climate in Norway	11
3.1.1 Historical	11
3.1.2 Future	12
3.2 Hydrological Modelling for Potential Hydropower	13
3.3 PEST Parameter Estimation	14
3.4 Different Versions of the HBV Model	14
4 Methodology	17
4.1 Study Area	18
4.2 Data	19
4.2.1 Data for Temperature and Precipitation	19
4.2.2 Data for Observed Temperature and Precipitation	21
4.2.3 Data for Observed Discharge	22
4.2.4 Data for Evaporation	22
4.3 Hydrological Modelling	23
4.3.1 HBV	23

4.4	Model Parameters	29
4.5	Model Calibration and Validation	30
4.6	Discharge to Potential Hydropower	31
4.7	Sources of Errors	31
5	Results and Discussion	33
5.1	Model Calibration and Validation	33
5.2	Optimized Parameters	39
5.3	Temperature and Precipitation	40
5.4	Annual Discharge	42
5.5	Monthly Discharge	45
5.6	Using the HBV Educational Version for Hydrological Modeling	49
5.7	Uncertainties	49
5.8	Limitations Related to the Datasets	50
5.9	Strengths and Weaknesses	51
5.10	Contribution to the Literature	52
6	Conclusions	53
7	Further Work	55
A	Climate Models	57
B	Extracting Data - Python Script	58
C	HBV Model - Python Script	60
D	HBV Model Calibration - Python Script	62
E	HBV Model Validation - Python Script	64
F	HBV Model Simulated Discharge - Python Script	65
	Bibliography	67

List of Figures

1.1	Global average surface temperature [1]	1
2.1	Simplified schematic of a hydroelectric power plant [16]	5
2.2	An example of Thiessen Polygon Method usage [18]	6
2.3	Global average surface temperature change (relative to 1986-2005) for different RCP scenarios [25]	10
4.1	A map of Agder County divided into its various watersheds. The area of interest in this study is area 4, Tovdalsvassdraget. [42]	18
4.2	Representation of the desired area. The red highlighted clipping area represents Tovdalsvassdraget in this study	20
4.3	The station Byglandsfjord-Solbakken represent the observed temperature for the area.	21
4.4	Stations Tovdal, Mykland, Dovland and Herefoss (dark green) represent the observed precipitation in the area.	21
4.5	The Flakksvann station (marked in red) represent the observed discharge for the area.	22
4.6	General processes of educational version of HBV model [24]	23
4.7	The process of modelling the effective precipitation [48]	25
4.8	The process of modelling soil moisture [48]	25
4.9	Relationship between soil moisture, field capacity, runoff coefficient and β [24]	26
4.10	Relationship between the actual evapotranspiration and PWP [24]	27
4.11	Conceptual reservoirs used to estimate runoff response [24]	28
5.1	Comparison of simulated and observed daily discharge for the year 1996 before calibration. The red line represent the simulated discharge while the blue line represent the observed discharge.	34
5.2	Comparison of simulated and observed daily discharge for the year 1996 after calibration. The red line represent the simulated discharge while the blue line represent the observed discharge.	34
5.3	Daily temperature year 1996	35
5.4	Daily precipitation year 1996	35
5.5	Snowpack year 1996	35
5.6	Soil moisture year 1996	35
5.7	Storage upper reservoir year 1996	36
5.8	Storage lower reservoir year 1996	36
5.9	Actual evapotranspiration year 1996	36
5.10	Effective precipitation year 1996	36
5.11	Comparison of simulated and observed daily discharge for the validation period. The red line represent the simulated discharge while the blue line represent the observed discharge.	37
5.12	Scatter plot showing the relationship between observed and simulated discharge values, with a linear regression line (red) and a reference line (black dotted) representing an ideal relationship	38

5.13	Yearly average temperature in Agder County displayed as the median of the climate models. The graphs are smoothed. The blue line represents the RCP4.5 scenario, while the red line represents the RCP8.5 scenario.	40
5.14	Projected percentage change in yearly average precipitation from 1971-2000 reference period for Agder County. The graphs are smoothed and shows the median of the climate models. Blue line represents RCP4.5 scenario while red line represents RCP8.5.	41
5.15	Estimated total annual discharge as a percentage change from the reference period of 1971-2000. The median of the climate models is used and smoothing is applied to the graphs to remove short-term variability. The shaded areas behind the lines represent variations among different climate models.	42
5.16	Different climate models used in the RCP4.5 scenario are shown as percentage changes from the reference period 1971-2100. The graph illustrates the wide range of projected changes in annual discharge among the different models. Smoothness is applied to remove short-term variability.	43
5.17	Different climate models used in the RCP8.5 scenario are shown as percentage changes from the reference period 1971-2100. The graph illustrates the wide range of projected changes in annual discharge among the different models. Smoothness is applied to remove short-term variability.	43
5.18	Monthly discharge changes from the reference period (1971-2000) for the mid-century period (2036-2065) under the RCP4.5 and RCP8.5 scenarios. The median of the climate models is used.	45
5.19	Monthly discharge changes from the reference period (1971-2000) for the late-century period (2071-2100) under the RCP4.5 and RCP8.5 scenarios. The median of the climate models is used.	46
5.20	Monthly discharge for RCP4.5 for mid and late-century. The blue line represents the mid-century, and the red line represents the late-century. The graphs show the percentage change from the reference period 1971-2000. The median of the climate models is used, and smoothing is applied to the graphs to remove short-term variability.	47
5.21	Monthly discharge for RCP8.5 for mid and late-century. The blue line represents the mid-century, and the red line represents the late-century. The graphs show the percentage change from the reference period 1971-2000. The median of the climate models is used, and smoothing is applied to the graphs to remove short-term variability.	47

List of Tables

2.1	Representative concentration pathways explanation [25]	9
4.1	Coordinates used to limit the dataset to the desired area	20
4.2	HBV parameters with ranges considered in the model	29
4.3	Initial values for running the model	29
4.4	Nash-Sutcliffe efficiency [49]	30
4.5	Pearson correlation coefficient [50]	31
5.1	Optimized parameters and their respective ranges	39
A.1	Overview of GCM/RCM combinations used from EURO-CORDEX [43]	57

Abbreviations

CORDEX	Coordinated Regional Climate Downscaling Experiment
EQM	Empirical Quantile Mapping Method
ESD	Empirical Statistical Downscaling
GA	Generic Algorithm
GCM	Global Climate Model
GIS	Geographic Information System
GUI	Graphical User Interface
HBV	Hydrologiska Byråns Vattenbalansavdelning
IPCC	Intergovernmental Panel on Climate Change
NVE	Norwegian Water Resources and Energy Directorate
QGIS	Quantum Geographic Information System
RCM	Regional Climate Model
RCP	Representative Concentration Pathway
SWAT	Soil and Water Assessment Tool
VIC	Variable Infiltration Capacity

Nomenclature

Symbol	Description	Unit
β	Model parameter	[mm]
ρ	Density of water	[kg/m ³]
A	Watershed area	[m ²]
C	Model parameter	[-]
DD	Degree-day correction factor	[-]
E_{a_i}	Actual evapotranspiration	[mm]
FC	Field capacity	[-]
g	Gravitational acceleration	[m/s ²]
H	Gross head	[m]
K_0	Near surface flow storage coefficient	[-]
K_1	Interflow storage coefficient	[-]
K_{perc}	Percolation storage coefficient	[-]
K_2	Groundwater storage coefficient	[-]
L	Threshold water level	[mm]
LW_i	Liquid water	[mm]
n	Number of time steps	[-]
P	Hydropower capacity	[W]
P_i	Precipitation	[mm]
P_{eff_i}	Effective precipitation	[mm]
PE_{a_i}	Adjusted potential evapotranspiration	[mm]
PE_{m_i}	Long term mean monthly potential evapotranspiration	[mm]
PWP	Soil permanent wilting point	[mm]

Q	Discharge	[m/s ³]
Q_{0_i}	Near surface flow	[m/s ³]
Q_{1_i}	Interflow	[m/s ³]
Q_{2_i}	Baseflow	[m/s ³]
Q_{perc_i}	Percolation	[m/s ³]
Q_{o_i}	Observed discharge	[m/s ³]
Q_{s_i}	Simulated discharge	[m/s ³]
\bar{Q}_{o_i}	Mean observed discharge	[m/s ³]
\bar{Q}_{s_i}	Mean simulated discharge	[m/s ³]
R_{NS}	Nash-Sutcliffe coefficient	[-]
R_P	Pearson correlation coefficient	[-]
$S1_i$	Upper reservoir water level	[mm]
$S1_{i-1}$	Upper reservoir water level the previous day	[mm]
$S2_i$	Lower reservoir water level	[mm]
$S2_{i-1}$	Lower reservoir water level the previous day	[mm]
S_{m_i}	Snowmelt rate water equivalent	[mm]
SM_i	Actual soil moisture	[mm]
SM_{i-1}	Actual soil moisture the previous day	[mm]
SP_i	Snowpack	[mm]
SP_{i-1}	Snowpack previous day	[mm]
T_i	Mean daily air temperature	[°C]
T_{m_i}	Long term mean monthly temperature	[°C]
T_t	Threshold temperature	[°C]

Chapter 1

Introduction

Today, climate change is the greatest challenge in all parts of the world. It is widely acknowledged that the rise in human-induced greenhouse gas emissions is a major contributor to the increase in global temperature, alterations in precipitation and weather patterns. These changes have already impacted life on Earth and will continue to have significant consequences in the future.

One of the most obvious effects of climate change is the increase in global temperature. Figure 1.1 shows the yearly global surface temperature compared to the average from 1880 to 2022. Since the 1800s, the Earth has warmed by an average of 1 °C, and it is expected to increase even more [1]. Increased temperatures lead to the melting of glaciers and ice caps, which in turn leads to rising sea levels and an increased risk of flooding in coastal areas. Changes in precipitation patterns are also a consequence of climate change. While some areas may experience increased rainfall, others may experience drought and water scarcity, as observed in Italy this year and in previous years [2]. Changes in precipitation can lead to flooding, soil erosion, crop failure and food shortages. In some areas, changes in precipitation can also affect the availability of clean water. The water supply is critical for many big cities worldwide, thereby having implications for health and well-being. Johannesburg in South Africa is a well-known example of this [3].

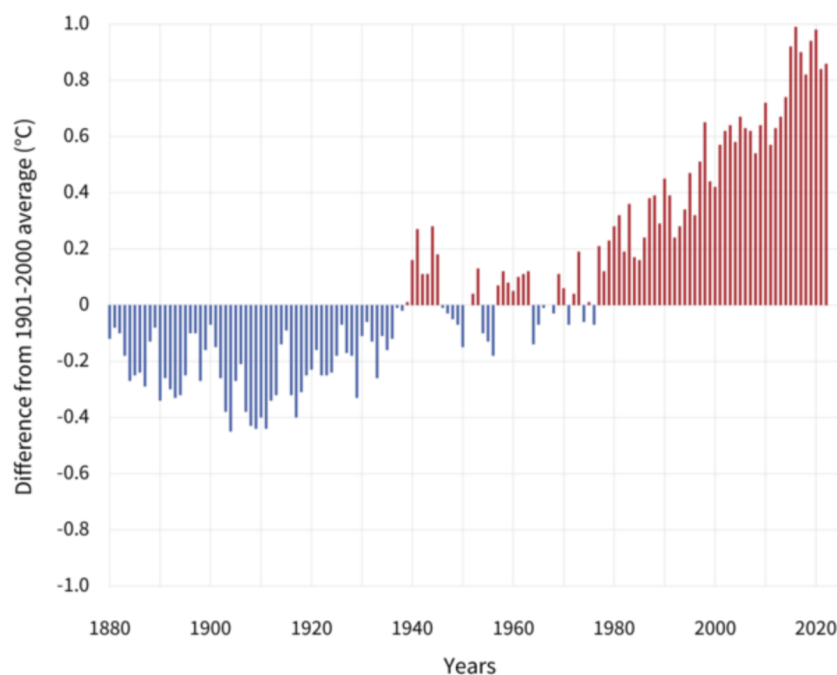


Figure 1.1: Global average surface temperature [1]

As the effects of climate change become more apparent, people around the world are facing a variety of challenges. Climate change is causing the melting of the ice in the polar areas, Greenland and the enormous glaciers in different parts of the globe. The sea level is already rising, and some small islands in the Pacific Ocean and the Indian Sea are about to be flooded [4]. Densely overpopulated areas like the Benelux and Bangladesh will be uninhabitable [5] [6]. This will add to the migration of people to the already increasing migration of people. One group that is particularly vulnerable to the effects of climate change is the Inuit people of Greenland [7]. Ice melting is causing changes in ocean currents, affecting fish populations and making it more difficult for the Inuit people to catch the fish and whales they rely on for food. The Inuit people also have a deep connection to the land and the environment, and their traditional way of life is intimately tied to the natural world. As climate change alters the landscape and disrupts traditional patterns of life, the Inuit people risk losing a fundamental part of their cultural heritage. They share this loss with millions of people worldwide who are affected by climate change in one way or another.

Taking action on climate change is necessary for the world to achieve its climate goals. Reducing greenhouse gas emissions is essential to achieve these goals. Utilizing renewable energy, improving energy efficiency, capturing and storing carbon dioxide, and changing production and consumption patterns are some ways to limit these emissions. Adapting to the changes that have already occurred and strengthening resilience to extreme weather events and natural disasters are equally important. Several agreements have been made worldwide to achieve various climate goals for the future. One is the Paris Agreement developed by The United Nations in 2015 [8]. The agreement consists of all countries being obliged to cut greenhouse gases and adapt to climate change, and that the temperature on Earth must not rise by more than two degrees Celsius before the end of the century. All countries must also have a clear plan for managing this. The United Nations also has several Sustainable Development Goals, where the 7th goal reads as follows: *Ensure access to affordable, reliable, sustainable and modern energy for all* [9]. Clean energy refers to energy generated from a natural source that is continually renewed. Climate agreements are crucial in mitigating climate change, which is urgently needed. Taking part in these agreements contributes to reducing greenhouse gas emissions, adapting to climate change and transitioning to a low-carbon economy. As such, these agreements represent a critical effort to protect our planet and ensure a more sustainable future for generations to come.

Hydropower is the most commonly used form of renewable energy in several countries, including Norway. It represents about 17% of global electricity production. In Norway, hydropower is the primary source of electricity, accounting for about 90% of the country's electricity production [10]. This makes Norway one of the most hydro-dependent nations globally. However, this high dependency raises an interesting question about climate change's impact on future hydropower production. Increased temperatures can cause increased evaporation, while changes in precipitation patterns can lead to drought periods that reduce water availability. This can result in reduced power production and increased pressure on water resources. Increased precipitation can also cause flooding due to heavy rainfall. This can lead to the destruction of infrastructure and equipment used in hydropower plants, as well as reduced access to water resources.

Agder County is the southernmost county in Norway, formed by merging the two former counties of Aust-Agder and Vest-Agder in 2020. The county is known for the sunniest and warmest climate in the country. According to The Norwegian Water Resources and Energy Directorate's (NVE's) overview of power plants in Norway, total hydropower production in Agder County is about 14.6 TWh referred to the inflow period 1991-2020, which amounts to 10.66% of total Norwegian hydropower production referred to the same inflow series [11]. There are plans for several new hydropower projects in this area. Based on currently avail-

able information, a combination of larger projects, potential upgrades and expansions of existing larger hydropower plants, small-scale hydropower development and environmentally sound design of waterways could result in an estimated increase in production of approximately 500-700 GWh/year in Agder County [12]. This includes the Fennefoss power plant, Syrtveit power plant, Øygard and Kvernevatn power plants, Knaben-Solliåna, Mandalselva and various small-scale private power plant developments.

The significant increase in temperature and precipitation around the world has led to changes in the hydrological cycle, affecting the hydropower potential. This has raised concerns about the long-term viability of this energy source, and therefore, it is essential to evaluate the potential impact of climate change on hydropower production. Numerous studies have been conducted worldwide, both on a global scale and in different countries and regions. Hisdal et al. (2010) and Wilson et al. (2010) studied how the streamflow has changed over the last century in the Nordic countries. They both conclude that temperature and precipitation changes are why the streamflow has changed. Holmqvist (2014) studied the Norwegian water balance and concluded that the changes in streamflow also apply to Norway. Roald et al. (2006) investigated the impact of climate change on streamflow in Norway from 1971 to 2100, while Hanssen-Bauer et al. (2015) examined the hydrology over the next century. Both conclude that climate change will significantly impact the years ahead. Hydrological modeling is a crucial tool for assessing hydropower's future potential. Various hydrological models are available, each with its advantages and disadvantages. The choice of model depends on the challenges in the area being investigated and the available data. Hydrologiska Byråns Vattenbalansavdelning-modellen (HBV) is the hydrological model most used for simulations in Norway. Several versions of the HBV model have been developed in addition to the original, some with simplifications for easier understanding.

1.1 Research Question

In recent years there has been increased attention to hydropower due to its ability to mitigate climate change. The impact of climate change on hydropower remains uncertain, with different regions experiencing different risks and benefits. Agder County is home to several hydropower plants and is expected to be particularly vulnerable to climate change impacts, including rising temperatures, changes in precipitation patterns and increased frequency and intensity of extreme weather events. As temperatures continue to increase, there will be a reduction in the amount of snowfall during winter, leading to a gradual release of the natural snow reservoir during spring. This thesis's main objective is to assess climate change's impact on hydropower potential in Agder County over the next century. Specifically, this thesis aims to answer the following research question:

How will hydropower potential in Agder County be affected by climate change over the next century?

To address this research question, an educational version of HBV will be used with future weather data obtained from global and regional climate models under different emission scenarios as input to estimate the future change in streamflow conditions. This thesis will also investigate the effectiveness of the educational version of HBV as a tool for addressing the research question. This will be addressed by comparing the model outputs with the observed discharge data from the study area. The results will provide insights into the capability of the educational version of HBV under different emission scenarios. The findings of this study will contribute to a better understanding of the potential risks and opportunities associated with hydropower production in the face of climate change during the next century.

1.2 Structure

The thesis is organized into several chapters, each with a specific focus. Chapter 2 provides an overview of the theoretical background related to the topic. Chapter 3 reviews previous publications related to hydrological conditions and hydrological modeling. Chapter 4 presents the methodology for deriving the data and describes how the hydrological modeling has been conducted. Chapter 5 presents the results and discusses the uncertainties, limitations and contributions to the literature. A conclusion is drawn in Chapter 6, summarizing the main findings and their significance. Chapter 7 provides recommendations to further work related to the study.

Chapter 2

Theory

This chapter explains the theory mentioned throughout the thesis. The presented theory provides the basis for several preconditions.

2.1 Potential Hydropower

Hydropower potential can be divided into three categories: gross theoretical potential, technical potential and economically feasible potential. Gross theoretical potential refers to the theoretical maximum amount of energy that can be produced by using all available water resources in a region [13]. Technical potential refers to the hydropower capacity that is attractive and easily accessible with current technology. The economically feasible potential of a site is the amount of hydropower generating capacity that can be built after evaluating the site's feasibility at current prices. [14] The power that a stream can generate depends on two factors [15]:

- The height difference between the water level at the upstream reservoir and the water level at the discharge, measured in meters (m), is called the gross head (see Figure 2.1). The greater the head, the more powerful the stream.
- The discharge (m^3/s) represents the volume of water that passes by a fixed point in one second.

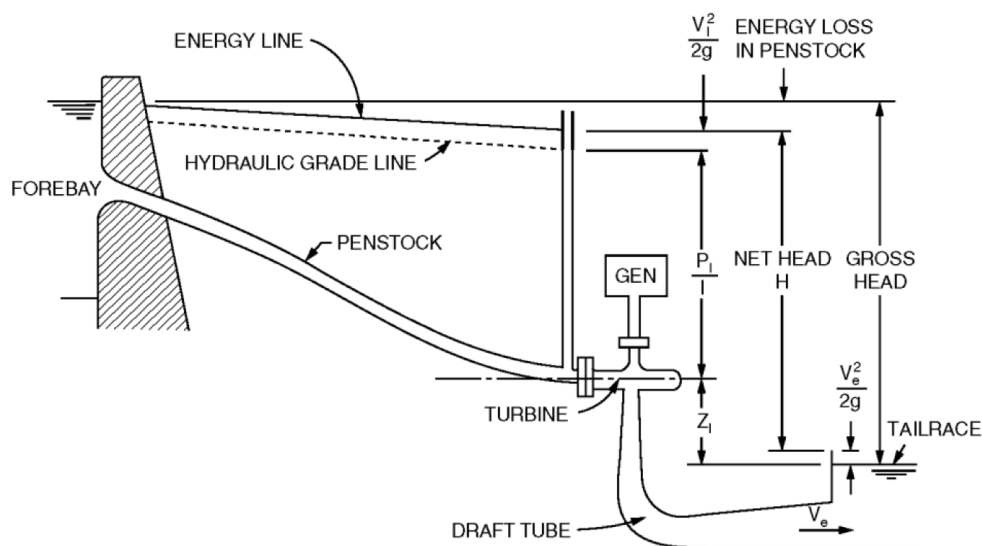


Figure 2.1: Simplified schematic of a hydroelectric power plant [16]

The gross theoretical potential is typically used in studies because it estimates the maximum energy that could be generated from water resources, without considering limitations and constraints that may affect a project’s technical and economic feasibility. The gross potential hydropower can be calculated using Equation 2.1:

$$P = Q \cdot H \cdot \rho \cdot g \quad (2.1)$$

where P is the hydropower capacity (W), Q is the discharge (m^3/s), H is the gross head (m), ρ is the density of water ($1000 \text{ kg}/\text{m}^3$) and g is the gravitational acceleration ($9.81 \text{ m}/\text{s}^2$).

2.2 Thiessen Polygon Method

The Thiessen Polygon Method divides a geographic area into smaller sections based on the proximity of a set of known points, such as rain gauges. This method is helpful for hydrologic studies because precipitation is typically measured at specific points. The goal is often to evaluate precipitation over a larger area, like a catchment or drainage basin. [17]

To begin the Thiessen Polygon Method, rain gauges inside or near the catchment area must be identified. On a map, the locations of each rain gauge are plotted along with the amount of precipitation measured. Each rain gauge is then connected to its nearest neighbors with straight lines, creating a series of triangles. Each line is bisected perpendicularly until it intersects with another bisected line, creating an irregular polygon. The polygons represent the influence area for a specific rain gauge, with precipitation within each polygon representing the amount measured at the gauge. The total precipitation over a catchment area can be estimated by calculating a weighted average of the precipitation measured at each rain gauge. [18]

Even though the Thiessen Polygon Method assumes that each point within its polygon is equally influential and that its boundaries are not affected by environmental conditions, it is still widely used in GIS (geographic information system) analysis because it can be used to estimate the spatial distribution of a variable over a large area simply and efficiently. [19]

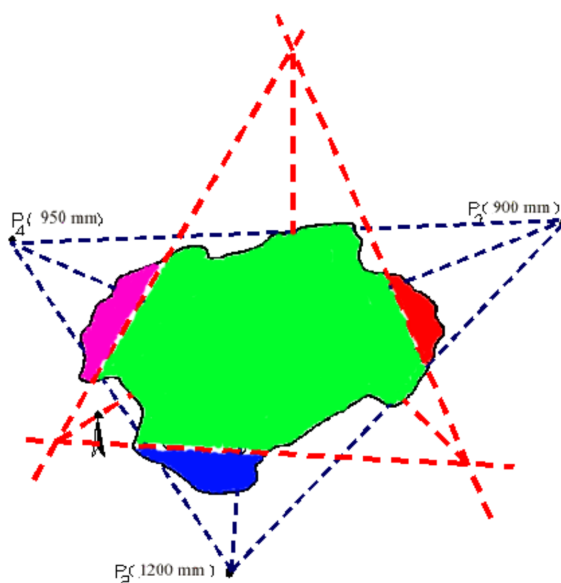


Figure 2.2: An example of Thiessen Polygon Method usage [18]

2.3 Hydrological Models

Hydrological models are crucial for evaluating future hydropower potential by providing valuable insights into water availability, runoff and overall energy potential. These models are designed to achieve one of two primary objectives: to study system operation or to predict system behavior. Various hydrological processes, such as precipitation, snowmelt, evapotranspiration and infiltration, are incorporated into representations of the hydrological cycle. Hydrological models can determine how much energy can be generated by hydropower at a particular location based on the amount of water available. [20]

A hydrological model is essential for assessing future streamflow conditions in reservoirs and evaluating the effects of climate and land-use change on watersheds. The use of these models is critical to making informed hydropower development decisions when there is little data available or when hydrological systems are complicated. Hydrological models must consider several factors, including climate change, to evaluate future hydropower potential. With changes in precipitation patterns and increased temperatures, climate change will significantly impact water availability and hydropower potential.

Hydrological models are typically divided into three categories: empirical models, conceptual models and physically based models, which are explained in the following sub-sections. Data availability, watershed complexity, heterogeneity and model application are all factors that influence which approach is selected [20].

2.3.1 Empirical Models

Empirical models, also known as statistical models, describe data based on the observations made without the need for theoretical frameworks or assumptions about the underlying system. They aim to use past observations to predict future outcomes reliably. The primary advantage of empirical models is their simplicity, which makes them applicable in ungauged catchments without hydrological data. Empirical models can be applied in these catchments through regional analysis, which links model properties to the physical and climatic characteristics of the catchment. Therefore, empirical models are useful in areas with limited or no hydrological data. [20]

Empirical models are statistical models that focus on input-output relationships [21]. In the context of hydrology, these models use data on streamflow, temperature and precipitation to establish relationships between them. Despite being straightforward and user-friendly, the accuracy of these models can vary based on the conditions being modeled. Predictions generated by these models are simple and efficient, which is one of their main advantages. However, they may not always capture the complexity of the underlying hydrological system. In order to ensure their reliability, empirical models should be evaluated against observed data before being used for prediction purposes. [20]

2.3.2 Conceptual Models

Conceptual models are a type of hydrological model that provide a more comprehensive understanding of the underlying processes that influence streamflow. In conceptual models, watersheds are represented mathematically as interconnected storage reservoirs, which incorporate various components of hydrological processes. These models require a substantial amount of data to represent the system properly. Hence, their accuracy and availability depend on the input data. [20]

Conceptual models offer several benefits despite their complexity. When data is limited or hydropower potential has to be assessed quickly, it can be used to estimate water availability and runoff. These models can also be useful for decision-making processes where information about the hydrological system is limited or little knowledge exists. [22]

Conceptual models provide a more detailed view of the hydrological system, but assumptions and simplifications in constructing the model can limit their accuracy. Specifically, the lumped configuration of these models ignores spatial variation in parameter values across the entire watershed. Additionally, the models' accuracy heavily depends on the quality of the observed data used to calibrate them. [20]

2.3.3 Physically Based Models

A physically based hydrological model simulates precipitation, evaporation, infiltration and runoff using physical principles. Simulations of the hydrological system are based on differential equations that describe the laws of mass, energy and momentum conservation [20]. The runoff can be continuously simulated in physically based models by considering the spatial variability of land use and soil. [23] [21]

Physically based models provide a more detailed understanding of the hydrological system, but require significant input data and computational resources. They are especially useful for studying complex hydrological systems and can be applied to various spatial scales, from small catchments to large river basins [24]. The accuracy of physically based models depends heavily on the quality of the input data used, such as climate data, soil properties and land use characteristics. Furthermore, the models can be computationally demanding and require significant time and resources.

2.4 Representative Concentration Pathways

The Representative Concentration Pathways (RCPs) presented in the fifth assessment report of the Intergovernmental Panel on Climate Change (IPCC) are essential for predicting the potential impact of greenhouse gas emissions on the Earth's climate system. These scenarios are based on assumptions about future population growth, economic development, energy use and technological advances. The RCPs are used to explore possible futures and assess the potential impacts of different emissions paths on the Earth's climate system. [25] The emission scenarios presented by IPCC are listed and explained in Table 2.1.

Table 2.1: Representative concentration pathways explanation [25]

Scenario	Explanation
RCP2.6	This scenario assumes that the world's emissions peak around 2020 and then rapidly decline, leading to a global temperature rise of 1.0 °C (0.3-1.7 °C) by the end of the 21st century.
RCP4.5	This scenario assumes that emissions peak around 2040 and then decline gradually, leading to a global temperature rise of 1.8 °C (1.1-2.6 °C) by the end of the 21st century.
RCP6.0	This scenario assumes that emissions continue to rise throughout the 21st century before peaking in the mid- to late- century, leading to a global temperature rise of 2.2 °C (1.4-3.1 °C) by the end of the century.
RCP8.5	This scenario assumes that emissions continue to rise throughout the 21st century without any significant mitigation efforts, leading to a global temperature rise of 3.7 °C (2.6-4.8 °C) by the end of the century.

The RCPs are often used as inputs for climate and hydrological models. By running models with different RCPs, one can gain insights into how the Earth's climate will likely evolve and assess the potential risks and impacts of climate change. The RCPs are an important tool for researchers in assessing climate change's potential risks and impacts and identifying strategies to mitigate and adapt to its effects. They provide a framework for exploring different emissions scenarios, assessing their potential impacts on the Earth's climate system, and guiding decision-making in the years ahead.

The two most widely used scenarios in climate research are RCP4.5 and RCP8.5. RCP4.5 is an intermediate emissions scenario. As a result of this scenario, the radiative forcing should stabilize shortly after 2100, making it necessary to reduce emissions dramatically. RCP4.5 is defined by lower energy intensity, reforestation programs, and decreased use of croplands and grasslands due to yield increases and dietary changes. In addition, it assumes that aggressive climate policies will be implemented and methane emissions will be stabilized. CO₂ emissions only increase slightly before declining around 2040. RCP8.5 is a high-emission scenario, also called the "worst-case scenario". This scenario assumes no policy changes will be made to reduce greenhouse gas emissions. A future with increasing greenhouse gas emissions and high concentrations is predicted by RCP8.5. The scenario predicts three times today's CO₂ emissions by 2100, a rapid increase in methane emissions and increased use of croplands and grasslands driven by population growth. By 2100, it is estimated in this scenario that the world's population will be 12 billion. [26]

Figure 2.3 shows the global average surface temperature change relative to 1986-2005. There are two scenarios plotted, RCP 2.6 (blue) and RCP8.5 (red). The shaded areas indicate the level of uncertainty. This is a common way of presenting different scenarios for the future. Additionally, colored vertical bars for four scenarios indicate the mean and associated uncertainties in the period 2081-2100. [25]

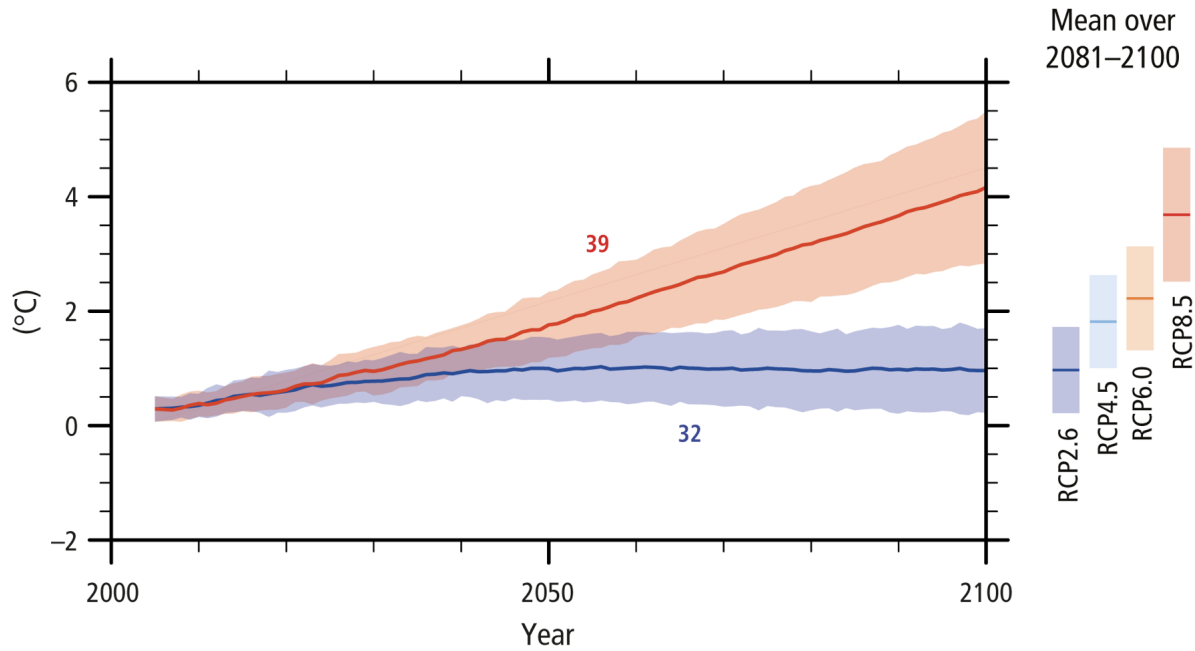


Figure 2.3: Global average surface temperature change (relative to 1986-2005) for different RCP scenarios [25]

Chapter 3

Previous Studies

3.1 Climate in Norway

Multiple studies have been conducted on whether climate change is advancing in Norway and how it will affect the future. This sub-chapter presents various studies on how Norway's climate has evolved and how it is likely to change in the next century. Climate change affects weather conditions, such as temperature and precipitation, affecting streamflow. The hydropower potential is significantly affected by this.

3.1.1 Historical

For the historical climate, Hisdal et al. (2010) investigated how the streamflow has changed in the Nordic countries in the last century. The study found that the streamflow during winter months has increased due to warmer temperatures and increased precipitation levels. Additionally, the streamflow has also increased in the springtime due to an earlier spring flood, which is evident in areas with both snowmelt and rain floods during spring. However, in summer, the streamflow has reduced, and more severe droughts have increased due to earlier snowmelt and increased evaporation from higher temperatures. The study acknowledges that the period analyzed and the selection of stations influenced the regional patterns found. However, trends toward increased streamflow dominated annual values and the winter and spring seasons. Trends in summer flow highly depended on the period analyzed, and no trend was found for the autumn season. The study also found a signal towards earlier snowmelt floods and a tendency toward more severe summer droughts in southern Norway. [27]

Wilson et al. (2010) have analyzed the trends in streamflow in the Nordic countries. The study found that the increase in streamflow during the winter and spring seasons was relatively higher than the increase in annual flows, indicating the influence of temperature on the timing of snowmelt and the seasonal distribution of flows. Changes in the timing of spring floods, except in Iceland, were also observed due to changes in snowmelt timing. In addition, the study found a tendency towards more severe summer droughts in southern and western Norway. The observed changes in streamflow in the Nordic countries are consistent with the estimated consequences of a projected temperature increase. The trends in annual and seasonal streamflow, floods, and droughts resulting from the changes in temperature and precipitation were found to depend on the period analyzed. However, they concluded that the streamflow in the Nordic countries has changed. These changes result from temperature-induced influences that have affected the timing of snowmelt and the seasonal distribution of flows. [28] Through Holmqvist's (2014) study regarding Norway's water balance from 1958 to 2012, he concludes that this trend also applies to Norway. [29]

3.1.2 Future

For future climate and hydrology, Roald et al. (2006) conducted a study to investigate the potential impacts of climate change on streamflow in Norway from 2071 to 2100. The study utilized a hydrological model that used data from three adjacent climate stations to assign daily time series of daily temperature and precipitation to each $1 \times 1 \text{ km}^2$ grid cell. The study found that there would be moderate changes in the annual streamflow, with some basins in East Norway experiencing a decline in some scenarios and an increase in most basins exposed to westerly winds. There would be significant changes in the seasonal distribution of streamflow. The winter season would experience an increase in streamflow throughout the country. The spring season would see an increase in mountainous basins in North Norway and a moderate decline in low-lying basins in the South and Mid-Norway. In the summer season, there would be a decrease in streamflow throughout the country. Given the moderate scenario, almost the entire country would experience an increase in streamflow in autumn. However, low-lying basins in the east and south would see a decrease in streamflow given the more extreme scenario. [30]

Hanssen-Bauer et al. (2015) investigated the impact of two climate scenarios, RCP4.5 and RCP8.5, on hydrology in Norway. The degree of change in hydrological conditions depends on the level of greenhouse gas emissions and subsequent atmospheric temperature increases. Under scenario RCP4.5, an increase of 1.8°C is predicted within 2031-2060, while scenario RCP8.5 will lead to an increase of 2.4°C in the same period. The increased temperature will also lead to more evaporation, which will offset the effect of increased precipitation on runoff values. Across the country, average temperatures are expected to increase, with northern regions experiencing the highest increase in temperature. Winters will become milder, summers warmer, and heat waves more frequent and intense. However, extreme cold events may still occur, particularly inland. Precipitation patterns are also likely to change, with an overall increase in most areas. Both scenarios will result in an increase in precipitation for all seasons, but RCP8.5 will cause a more significant increase than RCP4.5. The timing and intensity of precipitation changes may affect water availability for agriculture by causing increased flooding and decreased soil moisture. Runoff projections indicate a 3% increase for RCP4.5 and a 7% increase for RCP8.5. The report notes that extreme weather events such as heavy rainfall, storms and floods will likely become more frequent and intense, posing risks to infrastructure and settlements. Sea level rise is projected to continue, exacerbating coastal flooding and erosion. The report also discusses the impact of climate change on different sectors in Norway. The energy sector may be affected by changes in hydropower generation due to changes in water availability and snowmelt patterns. [31]

Based on Hanssen-Bauer et al. (2015), the Norwegian Climate Services Center presented a climate report for Agder County. The climate profile stated, among other things, that "Climate change will particularly lead to the need for adaptation to heavy precipitation and increased problems with surface water in Agder" [32]. The average annual temperature in Agder is estimated to increase by approximately 4.0°C , with the greatest increase in winter. Annual precipitation in Agder is estimated to increase by approximately 10%. [32]

Koestler et al. (2019) investigated the impact of climate change on the inflow of hydropower in Norway. The study found that the inflow has increased faster in recent decades than climate projections, and this increase applies to the whole country. On average, more inflow occurs in winter, but there is more variation from year to year. In contrast, there is less inflow during the summer, and the inflow from glacier melt will be significantly reduced towards the end of the century. However, the study also expects that the inflow will continue to increase in the future. In the RCP8.5 emission scenario, the inflow is projected to increase by about 7% by the end of the century due to increased temperature and precipitation, and

the south of Norway is expected to experience an inflow increase of over 10%. There is also variability in inflow from year to year, with the difference in inflow between Norway's driest and wettest winters being 26 TWh today, compared to 46 TWh at the turn of the century. [33]

3.2 Hydrological Modelling for Potential Hydropower

Over the past few decades, researchers from around the world have developed various effective methods for hydrological modeling. This sub-chapter provides an overview of some key findings and insights from previous studies using different hydrological models.

In Wang et al.'s (2018) study, a model-based approach was used to evaluate the effects of climate change on hydropower potential in China's Nanlijiang River Basin. They used the Variable Infiltration Capacity (VIC) hydrological model, calibrated and validated 1000 times. They found that it could simulate runoff well, but had greater uncertainty in low and high-flow simulations. Five climate models were employed, and the study analyzed the future spatial and temporal distributions of water resources. The findings revealed that changes in river discharge and water resource distributions are expected by 2100, resulting in an increase of 7.7% to 15.6% in hydropower potential under different RCP scenarios (2.6, 4.5, and 8.5). [34]

A study by Kouadio et al. (2022) examined the hydropower potential of the White Bandama Watershed in northern Côte d'Ivoire (West Africa). The hydrological model Soil and Water Assessment Tool (SWAT) was combined with Quantum Geographic Information System (QGIS) to evaluate water resource availability, hydropower potential and identify potential sites for future hydropower development. According to the results, the physical-based model had a good performance and is suited for future studies. However, during calibration and validation, the model underestimated peak flows at the hydrometric stations. In Ethiopia, a similar study was conducted by Dilnesa (2022) to identify potential hydropower sites in the Temcha watershed. Results agreed with Kouadio et al. (2022) that the use of the SWAT model in conjunction with a GIS tool was an effective method for identifying suitable sites for hydropower plants [35].

Rodric et al. (2021) aimed to investigate climate change's impact on the Lagdo dam's hydropower potential in the Benue River Basin, Northern Cameroon. The study used the HBV-Light hydrological model to simulate streamflow and compute hydropower potential based on the regional climate model's dynamically downscaled temperature and precipitation data. The data were obtained using the boundary conditions of two general circulation models (GCMs) and three Representative Concentrations Pathways (RCP2.6, RCP4.5, and RCP8.5). The results showed that hydropower potential in the Lagdo dam would be negatively affected under climate change scenarios, with a combination of decreased precipitation and streamflow and increased PET. The study concluded that climate change would decrease the hydropower potential of the Lagdo Dam in the future. The HBV-Light model was found to be highly performing during the calibration and validation stage, and the study used optimized model parameters. [36]

Bhattarai et al. (2017) used the HBV-Light model to estimate runoff and analyze changes in catchment hydrology and future flood magnitude due to climate change in the Narayani River Basin in Nepal, a snow-fed basin. The model was calibrated for 1995-2005 and validated for 2006-2008, with satisfactory results. The Nash-Sutcliffe coefficient during calibration ranged from 75.2% to 82.6%, and during validation ranged from 56.3% to 87.2% for all four sub-basins. The coefficient of determination (R^2) during calibration was between 0.789 and

0.844, and during validation was between 0.629 and 0.893. However, the model's structural complexity underestimated low flows, and some sharp peaks due to isolated precipitation events needed to be accurately estimated. The model showed an overall increase in monthly stream flow from January to June (34% to 51%) and November-December (10% to 15%) with the output of HADCM3 GCM, A1B scenario. Additionally, the sensitivity analysis indicated that global warming leading to an increase in average basin temperature would significantly increase the contribution to runoff from snowmelt. The model's performance is highly sensitive to the choice of parameter sets. Different parameters can provide the same efficiency, leading to ambiguity in determining the best parameter set. Therefore, generating a large number of parameter sets using the Monte Carlo method can prioritize important parameters to be used during calibration. [37]

The above studies are only a selection of the studies carried out in the field. There have been many studies regarding hydropower in various countries and worldwide. The choice of model may depend on the specific challenges in a given region or country, and what data are available to support the modelling.

3.3 PEST Parameter Estimation

Lawrence et al. (2009) studied the calibration of HBV hydrological models using PEST parameter estimation. They calibrated five best-fit models for each catchment based on observed streamflow and used the Nash-Sutcliffe criteria and volumetric bias as objective functions for model optimization. Fifteen HBV parameters were calibrated during the process. In their study, Lawrence et al. (2009) discovered that 90 catchments had model fits with N-S values greater than 0.70 for daily runoff, and 113 catchments had model fits with N-S values greater than 0.70 for weekly runoff. Additionally, the volumetric bias of the model was found to be less than $\pm 5\%$ in 105 catchments and less than $\pm 2\%$ in 56 catchments. The sensitivity analysis showed that the precipitation (rainfall) correction factor (PKORR) was the most sensitive parameter in 100 catchments. The second most sensitive parameter was found to be the precipitation (snowfall) correction factor (SKORR). These findings highlight the importance of high-quality precipitation input data. They also found that model calibrations with poorer fits were associated with smaller catchments in Norway's western and southwestern regions. The study showed that PEST parameter estimation effectively identified best-fit parameter sets for the HBV hydrological model. [38]

3.4 Different Versions of the HBV Model

Hanssen-Bauer et al. (2015) used a Norwegian-adapted version of the Swedish HBV model, developed at the Svenska Meteorologiska och Hydrologiska Institut (Bergström, 1976). HBV is the hydrological model most used for simulations and forecasts for streamflow in Norway [39]. Both Rodric et al. (2021) and Bhattarai et al. (2017) used HBV-light as a hydrological model when they explored the impact of climate change on the hydropower potential in their studies. There are many different versions of the HBV model software besides the original. HBV-light corresponds in principle to the version described by Bergström with only slight changes. In order to keep the software as simple as possible, several functions available in the SMHI version have not been implemented into HBV-light. [40]

An educational version of the HBV model have also been developed. The HBV - Education version, created by Amir AghaKouchak et al., is a hands-on tool that teaches the basics of hydrologic processes, model calibration and validation. The simplified conceptual model aims to provide an application-oriented learning environment that introduces hydrological processes. Through using this model, one can gain insights into how hydrological processes such as precipitation, snowmelt, soil moisture, evapotranspiration and runoff generation are interconnected. The educational HBV model is available as a MATLAB Graphical User Interface (GUI) or an Excel spreadsheet, making it accessible to many users [24] [41]. This study transposes the code to a Python script. By doing so, a Generic Algorithm (GA) can be used for calibration.

Chapter 4

Methodology

In this chapter, the methodology that guided this study is presented. The study area, Agder County, is profiled, and the processing of various datasets for use as input is described. Additionally, the hydrological model, which will be utilized for the simulations, is explained. First, a summary of the methodology is given for easier reading.

Summary of the Methodology

This study focuses on the Tovdalsvassdraget watershed in Agder County, Norway. A conceptual, educational version of the HBV model is used, which assumes that the area of interest is a single unit and that the parameters do not vary spatially across the watershed. The model uses temperature, precipitation and observed discharge as inputs to simulate the future discharge by utilizing physical concepts such as infiltration, snowmelt, evaporation and runoff. The model handles rainfall and snow based on temperature and evaluates how much rainfall contributes to runoff and soil moisture storage. The model's primary output is daily discharge values until 2100.

The HBV model demands calibration. The observed discharge used for calibration was from the station Flakksvann. The ranges for the model parameters are the ones recommended by Lawrence et al. (2009) [38], while initial values were set based on recommendations from Amir Aghakouchak, who created the educational version of HBV. The calibration period was from September 1980 to August 2000. For the validation, two joint periods from September 1972 to August 1980 and September 2000 to August 2004, together with the optimal values from the calibration were used.

The calibrated HBV model is simulated with precipitation and temperature data in a 1 km x 1 km grid from Global Climate Models (GCMs) and Regional Climate Models (RCMs), listed in Appendix A. These models are simulated during two climate scenarios; RCP4.5 and RCP8.5. The simulation output was simulated discharge converted to potential hydropower using Equation 2.1 in Chapter 2.1. This conversion allowed the estimation of the energy per net head that could be generated by a hydropower plant.

4.1 Study Area

This study focuses on Agder county, which is located in southern Norway. Agder county is known for its rugged terrain, abundance of rivers and lakes, and the country's sunniest and warmest climate. The county extends from the southern coastline to the northern mountainous regions of Bykle and Tokke, while the intermediate areas between the coast and the mountains are known for their woodland areas.

The study focuses explicitly on Tovdalsvassdraget, which can be found in area 4 of Figure 4.1. Tovdalsvassdraget was granted protected status in 1986 under the Verneplan III for watercourses (except for Uldalsvassdraget). This means that hydrological data can be studied without hydropower regulation.

For this study, Tovdalsvassdraget will be viewed as representative of Agder County. Tovdalsvassdraget spans a long distance from the northernmost region of the county to the south. Agder County's climate is characterized by temperate maritime conditions, resulting in mild winters and warm summers. The county receives a substantial amount of precipitation throughout the year. Due to the county's mountainous terrain and high precipitation levels, there is significant potential for hydropower. The county has a rich history of hydropower development, with many rivers and waterfalls utilized for electricity production.

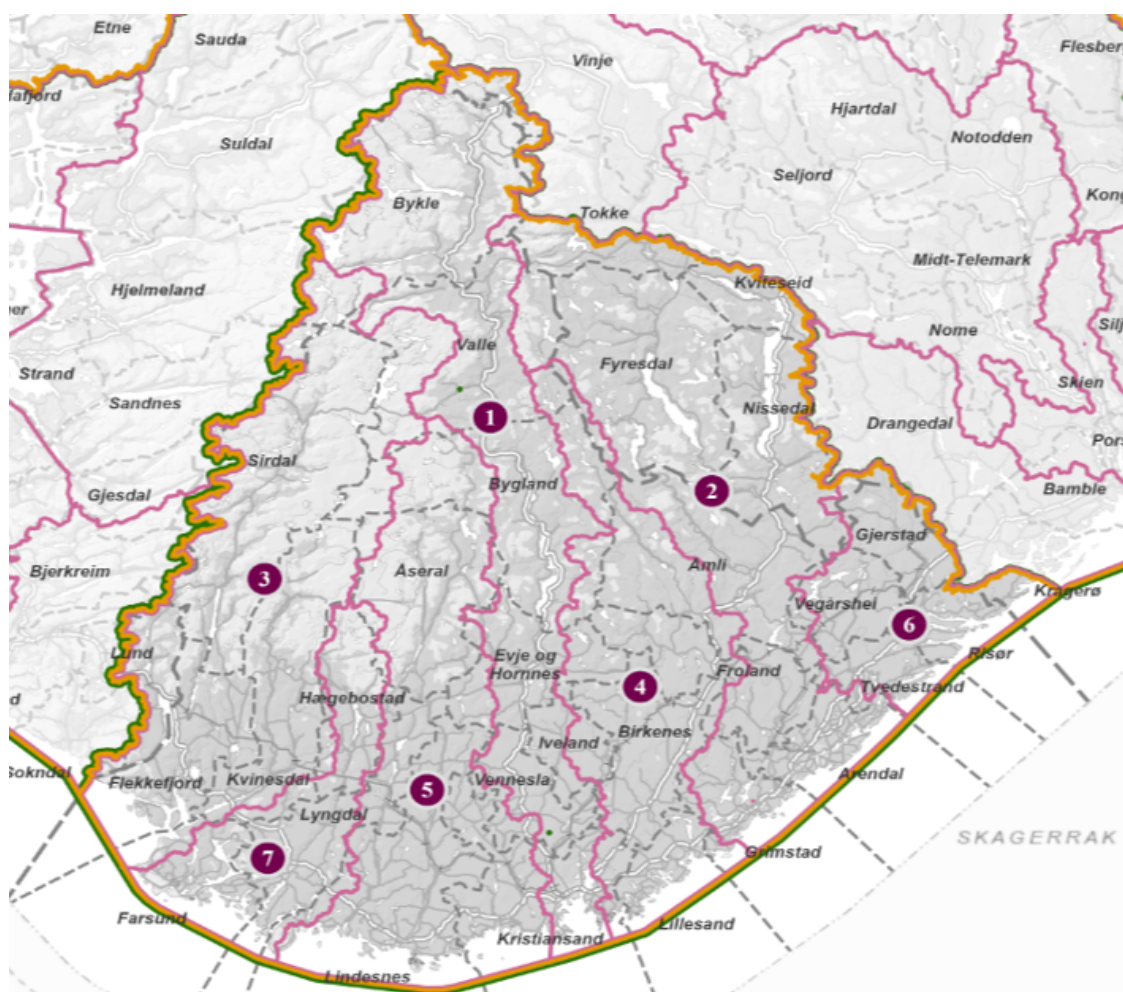


Figure 4.1: A map of Agder County divided into its various watersheds. The area of interest in this study is area 4, Tovdalsvassdraget. [42]

4.2 Data

In the further, a description of the datasets used for the simulations in this study is described. These datasets include observed data for temperature, precipitation, discharge and evaporation, as well as simulated datasets for temperature and precipitation. These data sets are necessary for the simulation and calibration of the hydrological model.

4.2.1 Data for Temperature and Precipitation

The data for temperature and precipitation in the simulations was obtained from the Norwegian Centre for Climate Service, a downloading page in collaboration with the NVE. The dataset used in this study consisted of temperature and precipitation values from 1971 to 2100 from ten different climate models (see Appendix A). The data were based on two climate scenarios, RCP4.5 and RCP8.5, specifically for Agder County. The downloaded dataset included a simulated historical period from 1971 to 2005 and a simulated future period from 2006 to 2100.

Data Construction

The dataset is used in several different studies. The first step of the data construction was done in “Climate in Norway 2100” by Hanssen-Bauer et al. (2015). The data was obtained from the Coordinated Regional Climate Downscaling Experiment (CORDEX), an international project to provide climate studies with data. The datasets were originally generated from simulations using Global Climate Models (GCMs) and had a gridded resolution of 100x100 km². The Euro-CORDEX subproject downscaled this data to a resolution of 12x12 km² using Regional Climate Models (RCMs). This utilized ten outputs with a resolution of 12x12 km² for RCP4.5 and RCP8.5, which were applied in the report “Climate in Norway 2100”. [31][43] [44]

Regional Climate Modelling (RCM) and empirical statistical downscaling (ESD) were applied to downscale the data to smaller grids. RCMs have smaller grids than GCMs, but are constructed similarly. Simulation results from GCMs were used in the RCM as input variables. Systematic biases often occur during dynamical downscaling, so the dataset was de-trended and bias-corrected using an empirical quantile mapping method (EQM) based on 'seNorge' precipitation and temperature gridded data as the 'observed' data. In order to downscale the data from 12.5x12.5 km² to 1x1 km², the data were re-gridded and re-scaled using the simple nearest neighbor method. Quality control was then performed to ensure that "hot spots" did not occur, and wet-day correction was carried out as RCM simulations often predict too high precipitation levels. [31]

The resulting bias-corrected and downscaled data was then processed in the HBV model using temperature and precipitation as input variables to generate hydrological variables [43]. Calibration of the model was necessary to achieve output variables that were as close to observational values as possible. [31] These temperature and precipitation data (from their simulations) are downloaded and used for this study.

Delineation of the Dataset

The dataset contains hydrological data associated with coordinates presented in netCDF format files for the catchment. A Python script was developed with help from Joao Leal to retrieve data for the desired area, see Appendix B. For simplicity, the selected region was defined by a rectangular shape in the script. The catchment is not a rectangle, but average values will be similar for the rectangle and the catchment. The rectangle was used to simplify the coordinate referencing without losing accuracy. The rectangle is shown in Figure 4.2, and was delimited by the coordinates listed in Table 4.1. The script extracts temperature and precipitation data for each model and scenario run and converts it into an Excel format.

Table 4.1: Coordinates used to limit the dataset to the desired area

Min longitude	8.09
Max longitude	8.4
Min latitude	58.3
Max latitude	59.15

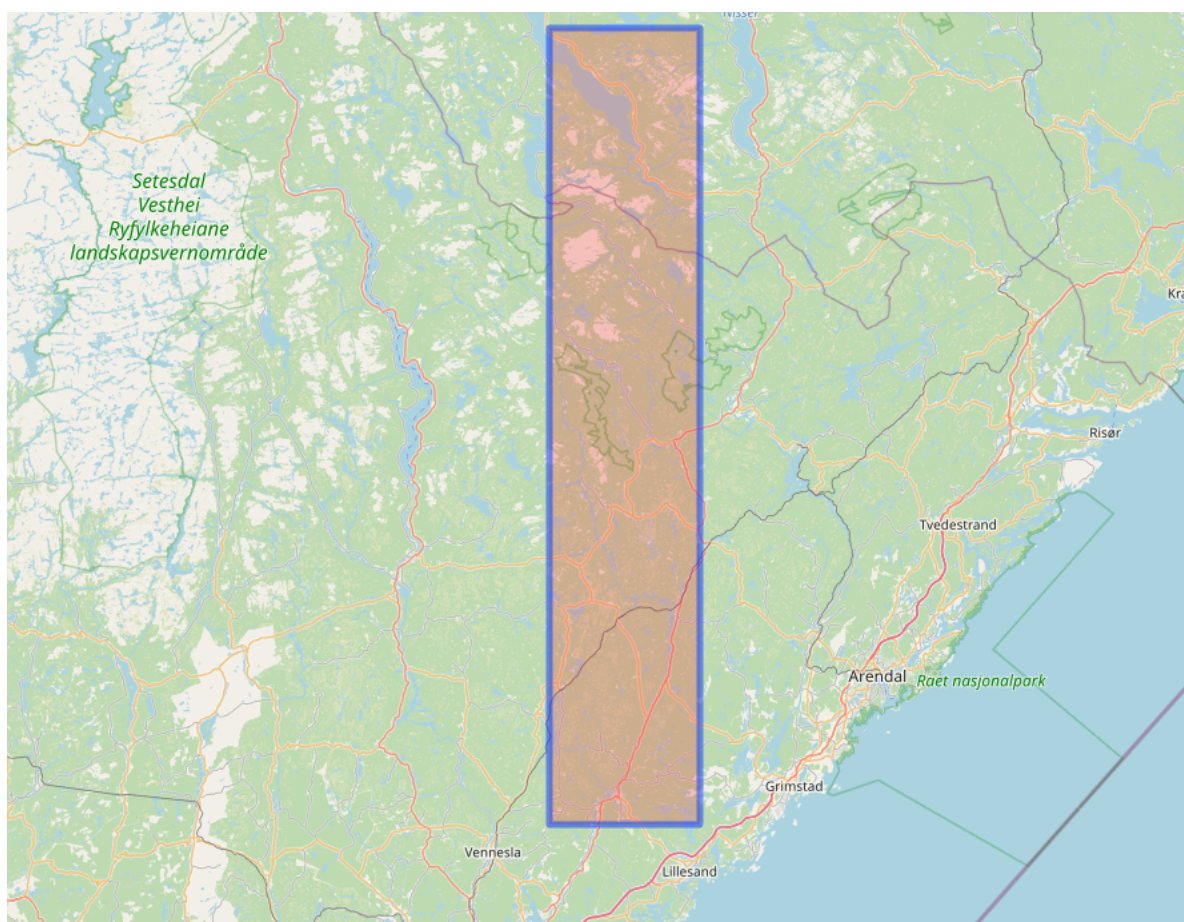


Figure 4.2: Representation of the desired area. The red highlighted clipping area represents Tovdalsvassdraget in this study

4.2.2 Data for Observed Temperature and Precipitation

To calibrate and validate the model, observed historical data for temperature and precipitation was downloaded from Seklima.no, a website that provides access to real data from various measuring stations. [45]. Actual observed temperature and precipitation data were utilized to obtain the most accurate representation of the resulting discharge.

For temperature, the mean temperature for each day from the station Byglandsfjord-Solbakken was used. The station can be seen in Figure 4.3. This station was used since it is the only station that measures air temperature nearby the desired area. The downloaded period was from January 1971 to December 2005, during which data was missing for nine days. These days were spread throughout the period, and therefore, interpolated values were used for those days. There were so few missing days in such a large time frame, so they were considered representative and not affecting the overall accuracy. A monthly average was calculated from the observed temperature data for the given period, which was required in the simulations. These average values were utilized in the simulations for the calibration, validation and historical period.

Nearby the catchment, four stations measured daily precipitation during the given period: Tovdal, Mykland, Dovland, and Herefoss. Figure 4.4 shows the four stations in a dark green color. To ensure the most representative results with four stations, only the years 1972 to 2004 were considered suitable for further use. There was too much missing data in 1971 and 2005 for one or more of the stations to allow for interpolation. The Thiessen polygon method (described in Chapter 2.2) was used to determine a value for each day in the area.

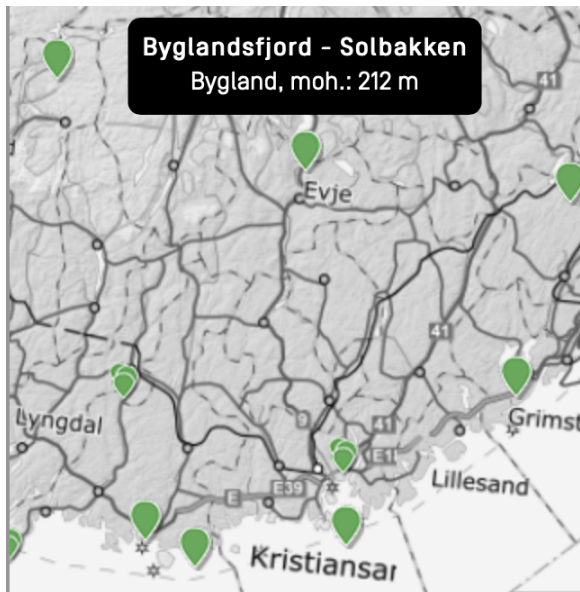


Figure 4.3: The station Byglandsfjord-Solbakken represent the observed temperature for the area.

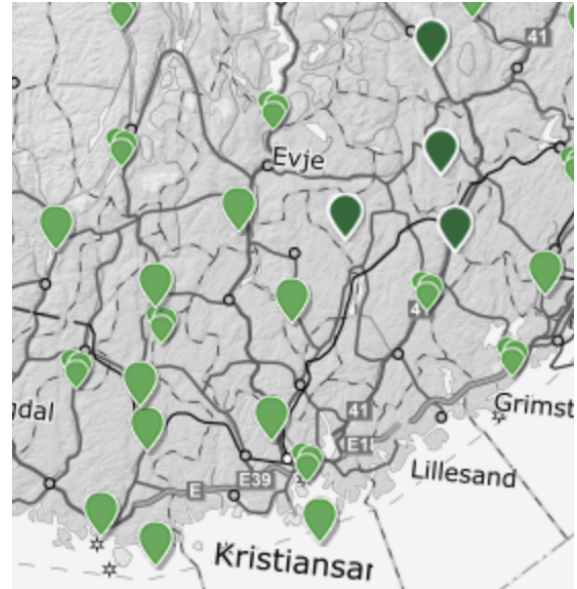


Figure 4.4: Stations Tovdal, Mykland, Dovland and Herefoss (dark green) represent the observed precipitation in the area.

4.2.3 Data for Observed Discharge

The observed discharge data was downloaded from Sildre, a source of current and historical hydrological information [46]. The Flakksvann station was selected as the representative for the entire area, and data were collected from January 1971 to December 2005. The Flakksvann station is located in Tovdalsvassdraget, meaning it does not have hydropower regulation.

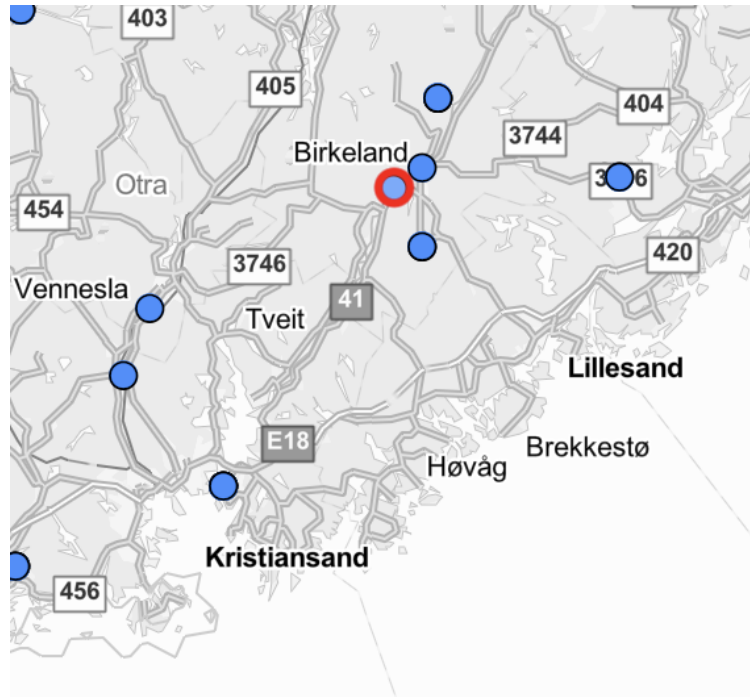


Figure 4.5: The Flakksvann station (marked in red) represent the observed discharge for the area.

4.2.4 Data for Evaporation

The data for long-term mean monthly potential evapotranspiration is obtained from Climate Engine. This tool uses Google Earth Engine for on-demand processing of satellite and climate data on a web browser [47]. The website allows the user to clip out the desired area for data. For this study, the entire Agder County was chosen. Mean evaporation was used from January 1971 to December 2005. After extracting the data, the average of each month for all years was used in the model.

4.3 Hydrological Modelling

In the further, a detailed overview of the hydrological model used in this study is provided. This includes its structure, parameterization, calibration and validation. The assumptions described reduce the number of parameters required for hydrological modeling.

4.3.1 HBV

This study used a conceptual model based on the HBV model due to its simplifications and easy implementation into a Python script. The educational version of the HBV model was used [24], initially available as an educational Excel spreadsheet or a Matlab script, but has been converted to a Python script for this study. The Python script was initially developed by Joao Leal as part of the process for this master's thesis, with subsequent modifications and completion by the author. The study uses a simplified spatially-lumped version of the model, which assumes that the area of interest is a single unit (zone) and that the parameters do not vary spatially across the watershed [24]. In Figure 4.6, the processes of the educational version of the HBV model are described.

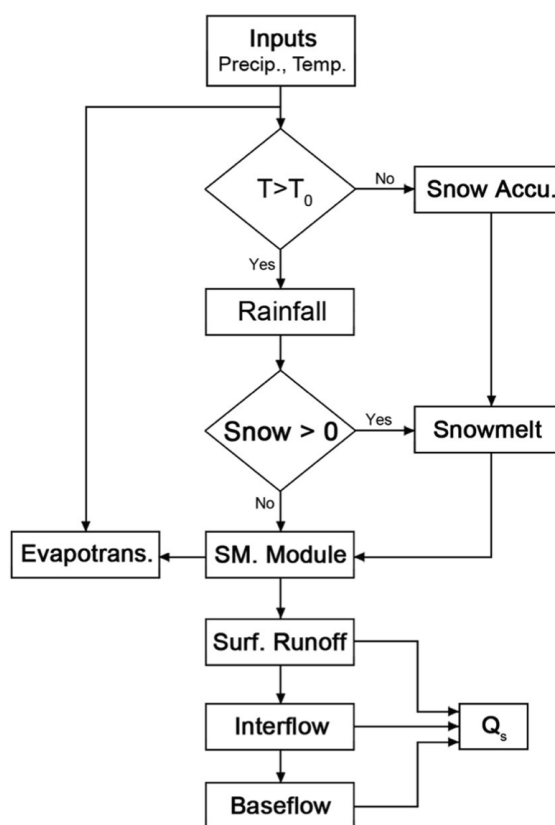


Figure 4.6: General processes of educational version of HBV model [24]

HBV is a hydrological model developed by the Swedish Meteorological and Hydrological Institute to simulate the hydrological cycle in a river basin. The HBV model is a conceptual model, as described in Chapter 2.3. The model uses temperature, precipitation and observed discharge as inputs to simulate the discharge by utilizing physical concepts such as infiltration, evaporation, snowmelt and runoff. As explained in Figure 4.6, the model handles rainfall and snow based on temperature, and evaluates how much rainfall contributes to runoff and soil moisture storage. The model's primary output is discharge at the watershed's outlet. The following sections provide descriptions of each module of the model and are implemented in the Python script in Appendix C.

Snowmelt and Snow Accumulation

The first step in the model is to separate precipitation into rainfall and snow, which requires an assumption. This study assumes that if the temperature is at or below the threshold temperature, all precipitation falls as snow. If the temperature is above the threshold, all precipitation falls as rainfall. This is expressed in the following equation:

$$\text{Precipitation} = \begin{cases} \text{Snow} & \text{if } T_i \leq T_t \\ \text{Rainfall} & \text{if } T_i > T_t \end{cases} \quad (4.1)$$

where T_i is the mean daily air temperature and T_t is the threshold temperature. In this study, the threshold temperature is one of the parameters estimated during calibration using ranges described in Chapter 4.4. Another important assumption is required regarding snowfall. If precipitation falls as snow, the assumption is that there will be neither infiltration nor direct runoff. This means that the precipitation will not immediately translate to runoff, but rather it will accumulate as snow until it melts. However, if the precipitation falls in the form of liquid water, the infiltration and direct runoff need to be calculated.

When snowfall occurs, it is essential to track snow accumulation and snowmelt. The model assumes that if the temperature remains below the threshold temperature, there will be no snowmelt. Once the temperature rises above the threshold temperature, snowmelt will begin. It is also assumed that if the accumulated snow is 0, there is no snowmelt, whatever is the temperature. This is expressed in Equation 4.2.

$$S_{m_i} = DD \cdot (T_i - T_t) \quad (4.2)$$

where S_{m_i} is the snowmelt rate water equivalent and DD is degree-day correction factor. The degree-day factor describes how much snow can melt per degree per day and is one of the parameters being optimized. Snow accumulation refers to the amount of snow accumulated on the ground, while snowpack is the total amount of snow accumulated on the ground over time. The snowpack is described as:

$$SP_i = \begin{cases} SP_{i-1} + P_i & \text{if } T_i < T_t \\ \max[SP_{i-1} - S_{m_i}, 0] & \text{if } T_i \geq T_t \end{cases} \quad (4.3)$$

where SP_i is the snowpack, SP_{i-1} is the snowpack the previous day, P_i is the precipitation.

Liquid Water, Effective Precipitation and Soil Moisture

The next step is to calculate the amount of liquid water in the system. In this study, liquid water refers to all available water in liquid form; rainfall and snowmelt. It is assumed that if the temperature is below the threshold temperature, the liquid water content is zero, indicating that everything is frozen. Conversely, if the temperature is above the threshold temperature, precipitation falls in the form of rain and snowmelt. If there is accumulated snow, snowmelt also adds. This is represented by the following equation:

$$LW_i = \begin{cases} 0 & \text{if } T_i < T_t \\ P_i + \min[SP_{i-1}, S_{m_i}] & \text{if } T_i \geq T_t \end{cases} \quad (4.4)$$

where LW_i is the liquid water.

The effective precipitation is illustrated in Figure 4.7. The field capacity (FC) represents the watershed's maximum soil moisture storage capacity. The soil moisture level can range from zero to the maximum field capacity. Hence, the field capacity serves as the upper limit for soil moisture. As the soil moisture level increases, the capacity for infiltration decreases and more liquid water contributes to direct runoff or effective precipitation. Equation 4.5 calculates the effective precipitation.

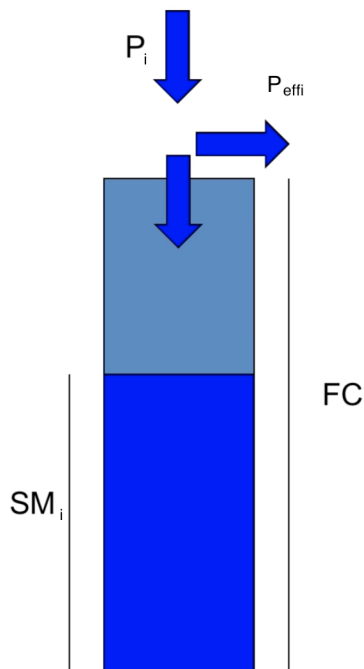


Figure 4.7: The process of modelling the effective precipitation [48]

$$P_{effi} = \left(\frac{SM_{i-1}}{FC}\right)^\beta LW_i \quad (4.5)$$

where P_{effi} is effective precipitation, SM_{i-1} is actual soil moisture the previous day and β is a model parameter (shape coefficient).

A water budget approach is employed for modeling the soil moisture module. The subsurface is conceptualized as a bucket where liquid water is an input. A proportion of the liquid water contributes to soil moisture, while the remaining contributes to direct runoff. The actual evapotranspiration represents a loss from the system as water evaporates from the soil and results in a decrease in soil moisture content. The process is illustrated in Figure 4.8 and the soil moisture is calculated using Equation 4.6.

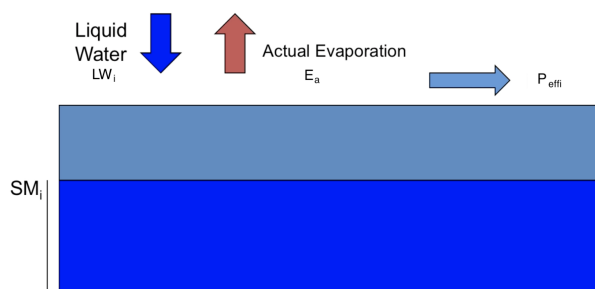


Figure 4.8: The process of modelling soil moisture [48]

$$SM_i = SM_{i-1} + LW_i - P_{eff_i} - E_{a_i} \quad (4.6)$$

where SM_i is the soil moisture and E_{a_i} is the actual evapotranspiration.

Figure 4.9 shows the relationship between soil moisture, field capacity, shape coefficient and runoff coefficient. By plotting the runoff coefficient against soil moisture, the role of beta (β) can be explored. The x-axis represents soil moisture, which ranges from zero to the field capacity. The runoff coefficient is generally less than 1. When β equals 1, the resulting line is linear, as the black dotted line shows. However, the graph exhibits non-linear behavior for higher values of β , such as 2 or 3. For a fixed amount of soil moisture represented by the vertical line, increasing β results in a decrease in the runoff coefficient. The parameter β controls the proportion of liquid water that contributes to runoff, allowing for adjustment of the amount of effective precipitation.

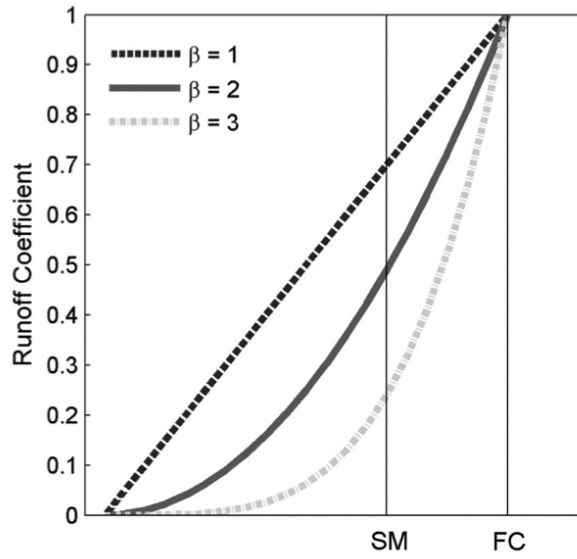


Figure 4.9: Relationship between soil moisture, field capacity, runoff coefficient and β [24]

Evapotranspiration

When calculating evapotranspiration, adjusted potential evapotranspiration is first determined. Potential evapotranspiration refers to the amount of water that can potentially evaporate, given sufficient water in the system and energy for evapotranspiration. Actual evapotranspiration, on the other hand, represents what actually happens. While the calculation is based on potential evapotranspiration, adjustments are made based on daily temperatures. The underlying assumption is that the long-term potential evapotranspiration is primarily influenced by long-term temperatures. Adjusted evapotranspiration is calculated using Equation 4.7:

$$PE_{a_i} = (1 + C(T_i - T_{m_i})) \cdot PE_{m_i} \quad (4.7)$$

where PE_{a_i} is adjusted potential evapotranspiration, T_{m_i} is long term mean monthly temperature, PE_{m_i} is long term mean monthly potential evapotranspiration and C is model parameter. The parameter C helps improve the model's performance when the daily temperature significantly differs from its long-term average.

Once the adjusted potential evapotranspiration is calculated, the actual evapotranspiration must be determined. Water availability in the system is a crucial factor in this regard. When sufficient water is available, the actual evapotranspiration is assumed to be equal to the potential evapotranspiration. However, if there is a scarcity of water in the system, the actual evapotranspiration needs to be estimated using a model parameter known as the permanent wilting point (PWP). The PWP serves as a threshold, and soil moisture below this point indicates water limitation. This is explained in the following equations:

$$E_{a_i} = \begin{cases} PE_{a_i} \left(\frac{SM_{i-1}}{PWP} \right) & \text{if } SM_{i-1} < PWP \\ PE_{a_i} & \text{if } SM_{i-1} \geq PWP \end{cases} \quad (4.8)$$

The graphical representation of the equations is shown in Figure 4.10, where the x-axis denotes soil moisture, and the y-axis represents actual evapotranspiration divided by adjusted potential evapotranspiration. If soil moisture exceeds the permanent wilting point, actual evapotranspiration equals adjusted potential evapotranspiration, resulting in a ratio of 1, represented by the horizontal line in the graph. On the other hand, if soil moisture falls below the permanent wilting point, the ratio changes linearly, as indicated by the upward slope of the line in the graph.

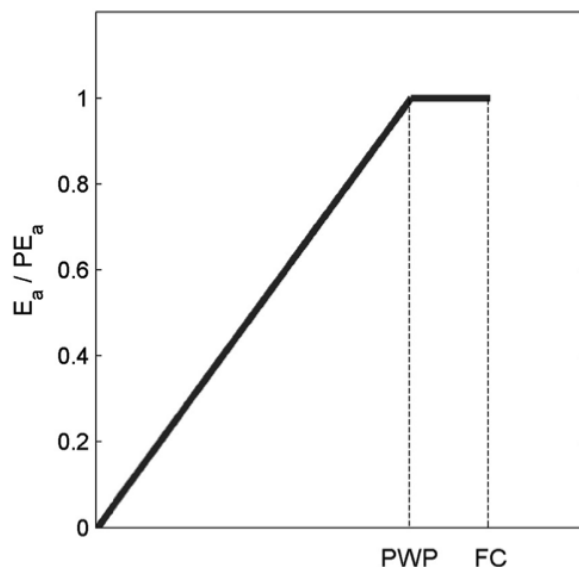


Figure 4.10: Relationship between the actual evapotranspiration and PWP [24]

Runoff Response

To calculate runoff, a bucket model approach is utilized, as it is a commonly used technique in conceptual hydrological modeling. Two separate buckets represent near-surface and sub-surface processes. The aim is to simulate the contributions of surface flow, interflow and base flow to the total runoff. A schematic representation in Figure 4.11 shows that the system comprises two conceptual reservoirs arranged vertically with one above the other. Q_{0_i} refers to the immediate and rapid contribution to runoff. When there is space for storage, water remains in the basin until it reaches a certain threshold, contributing to the overall runoff. However, the water will directly contribute to the runoff if the storage is already full.

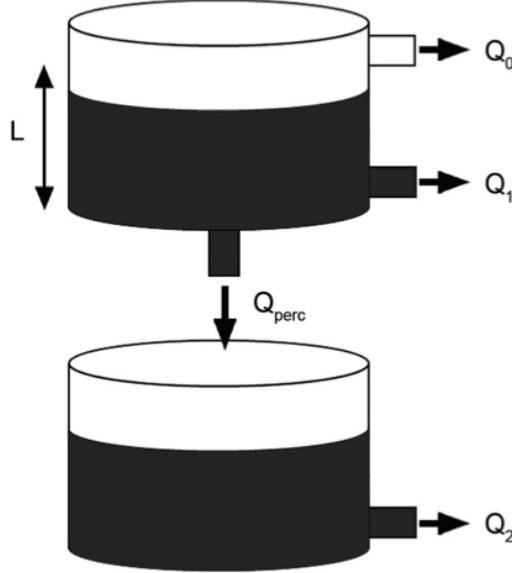


Figure 4.11: Conceptual reservoirs used to estimate runoff response [24]

The mass balance equations for the upper and lower reservoir is given by Equation 4.9 and Equation 4.10.

$$S1_i = S1_{i-1} + P_{eff_i} - Q_{0_i} - Q_{1_i} - Q_{perc_i} \quad (4.9)$$

$$S2_i = S2_{i-1} + Q_{perc_i} - Q_{2_i} \quad (4.10)$$

where $S1_i$ is the upper reservoir water level, $S1_{i-1}$ is the upper reservoir water level the previous day, $S2_i$ is the lower reservoir water level, $S2_{i-1}$ is the lower reservoir water level the previous day, Q_{0_i} is the near surface flow, Q_{1_i} is the interflow, Q_{2_i} is the baseflow and Q_{perc_i} is the percolation. Equations 4.11 to 4.14 are utilized to estimate outflows from the two conceptual reservoirs. The percolation equation connects the two reservoirs, while the remaining three equations will contribute to the calculation of overall runoff. Outflow is a function of storage, and if there is no storage, it is assumed that there will be no contribution to runoff. However, if water is present, a portion of it will contribute to the overall runoff.

$$Q_{0_i} = \begin{cases} K_0(S1_{i-1} - L) \cdot A & \text{if } S1_{i-1} > L \\ 0 & \text{if } S1_{i-1} \leq L \end{cases} \quad (4.11)$$

$$Q_{1_i} = K_1 \cdot S1_{i-1} \cdot A \quad (4.12)$$

$$Q_{perc_i} = K_{perc} \cdot S1_{i-1} \cdot A \quad (4.13)$$

$$Q_{2_i} = K_2 \cdot S2_{i-1} \cdot A \quad (4.14)$$

where K_0 is near surface flow storage coefficient, K_1 is interflow storage coefficient, K_{perc} is percolation storage coefficient, L is threshold water level and A is watershed area.

The total simulated discharge, Q_{si} , can be calculated by adding together the outflows from the first and second reservoirs, as Equation 4.15 shows:

$$Q_{si} = Q_{0i} + Q_{1i} + Q_{2i} \quad (4.15)$$

4.4 Model Parameters

For the model to run, model parameters and initial values were needed. In Table 4.2 the ranges of the HBV parameters used in this study are listed. The parameters' ranges are the ones recommended in PEST optimization [38]. There is a requirement that $PWP \leq FC$ is met during calibration.

Table 4.2: HBV parameters with ranges considered in the model

HBV Parameter	Description	Range considered
T_t	Threshold temperature	-1.0 - 2.0
DD	Degree day correction factor	1.0 - 5.0
FC	Field capacity	50.0 - 500.0
BETA	Shape coefficient	1.0 - 4.0
C	Model parameter for the adjusted potential evapotranspiration	0.01 - 0.1
K_0	Near surface flow storage coefficient	0.1 - 1.0
L	Threshold water level	10.0 - 100.0
K_1	Interflow storage coefficient	0.1 - 1.0
K_2	Groundwater storage coefficient	0.001 - 1.0
K_{perc}	Percolation storage coefficient	0.001 - 1.0
PWP	Soil permanent wilting point, defined as the minimum amount of water in the soil that the plant requires not to wilt (mm)	50.0 - 250.0

The initial values are listed in Table 4.3. These initial values are recommended by Amir Aghakouchak [48], the creator of the educational version of HBV. During the calibration and validation process, the simulation started in September, so the snowpack (SP) was set to 0. For simulations conducted afterward in January, SP was set to 25. This is a reasonable assumption since it is not unlikely that there would be some snow on the ground during this time of year.

Table 4.3: Initial values for running the model

Parameter	Description	Value
SP	Snowpack (mm)	0, 25
SM_i	Soil moisture (mm)	100
S1	Storage upper reservoir (fast response runoff) (mm)	2
S2	Storage lower reservoir (slow response runoff) (mm)	200

4.5 Model Calibration and Validation

Model calibration is a critical step in hydrological modeling to ensure accurate simulation results. The process involves adjusting model parameters to minimize the difference between observed and simulated hydrological data. For this model, the goal is to minimize the difference between observed and simulated discharge. To find the optimized parameters, Nash-Sutcliffe efficiency was evaluated:

$$R_{NS} = 1 - \frac{\sum_{t=1}^n (Q_{s_i}^t - Q_{o_i}^t)^2}{\sum_{t=1}^n (Q_{o_i}^t - \bar{Q}_{o_i})^2} \quad (4.16)$$

where R_{NS} is the Nash-Sutcliffe coefficient, Q_{s_i} is the simulated discharge, Q_{o_i} is the observed discharge, \bar{Q}_{o_i} is the mean observed discharge and n is the number of time steps. The Nash-Sutcliffe efficiency ranges from negative infinity to 1, where values closer to 1 indicate greater model accuracy.

To calibrate the model, data for temperature and precipitation described in Chapter 4.2.2 were used and compared to the observed discharge. September 1980 to August 2000 was used as the calibration period. The Python script in Appendix D is used for this process. This script uses GA to find the optimized parameters corresponding to the maximum Nash-Sutcliffe and saves the optimal results in CSV files. The model's performance is evaluated using Table 4.4.

Table 4.4: Nash-Sutcliffe efficiency [49]

Performance evaluation	Nash-Sutcliffe efficiency
Very good	$0.75 < R_{NS} \leq 1.00$
Good	$0.65 < R_{NS} < 0.75$
Satisfactory	$0.5 < R_{NS} < 0.65$
Unsatisfactory	$R_{NS} \leq 0.5$

For the validation, two joint periods from September 1972 to August 1980 and September 2000 to August 2004, together with the optimal values from the calibration, was used in the Python-script in Appendix E. For validation, both Nash-Sutcliffe efficiency and Pearson correlation coefficient are evaluated. The Pearson correlation coefficient is given by Equation 4.17 and the performance is evaluated by Table 4.5.

$$R_P = \frac{\sum_{t=1}^n (Q_{o_i}^t - \bar{Q}_{o_i}) \cdot \sum_{t=1}^n (Q_{s_i}^t - \bar{Q}_{s_i})}{\sqrt{\sum_{t=1}^n (Q_{o_i}^t - \bar{Q}_{o_i})^2} \cdot \sqrt{\sum_{t=1}^n (Q_{s_i}^t - \bar{Q}_{s_i})^2}} \quad (4.17)$$

where R_P is Pearson correlation coefficient and \bar{Q}_{s_i} is mean simulated discharge. Pearson correlation coefficients range from -1 to 1, with 1 indicating perfect linear agreement.

Table 4.5: Pearson correlation coefficient [50]

Correlation	Scale
Very high	$0.8 \leq r \leq 1.00$
High	$0.6 \leq r \leq 0.79$
Moderate	$0.4 \leq r \leq 0.59$
Low	$0.2 \leq r \leq 0.39$
Very low	$0 < r \leq 0.19$

4.6 Discharge to Potential Hydropower

The modeling process to estimate potential hydropower involved running simulations using different climate models and scenarios. The climate models used for simulation are listed in Appendix A, while the historical, RCP4.5 and RCP8.5 were the periods and scenarios used. The simulations were executed using the Python script in Appendix F, which must be manually adjusted for each climate model and scenario. The output of the simulations was a .csv file that contained the simulated discharge for each day in the period simulated.

To estimate the potential hydropower, the discharge data was converted using Equation 2.1 in Chapter 2.1, which calculates the energy that can be produced by a hydropower plant per unit of net head. This conversion allowed for the estimation of the energy that could be generated by a hydropower plant using the simulated discharge data.

4.7 Sources of Errors

Sources of error in this study can arise from various factors, some of which include:

- Data errors: It is possible that mistakes were made when the data were manually entered. Since this study involves human interaction, this is likely to occur.
- Data extraction: Inaccuracies can have occurred if the parameters are not correctly set up when extracting them from the database. This can have led to incorrect inputs being used.
- Shortcomings in the understanding of the climate system: Hydrological modeling is heavily dependent on the accuracy of climate data, and uncertainties in understanding the climate system can lead to errors in modeling results.
- Coding errors: When translating the educational version of the HBV model into a Python script, errors may have appeared.

Chapter 5

Results and Discussion

This chapter presents the study's results concerning the potential impacts of climate change on hydropower production in Agder County, Norway. To assess the potential impacts of climate change on hydropower production, an educational version of HBV was used to simulate the impact of changes in precipitation and temperature under different climate scenarios. In this chapter, the simulation results are given and the usability of the hydrological model is evaluated, with strengths and weaknesses.

The findings of this study can contribute for Agder County to better plan its energy future and adaptation to climate change. By providing insights into the potential impacts of climate change on hydropower production, the results can inform decisions related to energy infrastructure investments, renewable energy targets and climate adaptation strategies.

5.1 Model Calibration and Validation

Hydrological models are essential tools for understanding the behavior of watersheds and predicting the effects of different scenarios on their hydrological response. However, the accuracy of these models depends heavily on the calibration process, in which the model parameters are adjusted to best match the observed data. The available data was divided into two: a calibration period and a validation period. This study used the period from September 1980 to August 2000 as the calibration period. After calibration, the model was validated using two joint periods: September 1972 to August 1980 and September 2000 to August 2004, together with the optimal parameter values from the calibration period.

Figure 5.1 shows observed and simulated discharge before calibration, while Figure 5.2 shows the same data after calibration, specifically for 1996. In Figure 5.1, it is evident that the simulated discharge does not follow the trends of the observed discharge. In Figure 5.2, the correlation between simulated and observed discharge is considerably improved. After calibration, the simulated discharge follows the trends of the observed discharge more closely, but there are still some areas where the model struggles to replicate the observed discharge. Specifically, it appears that the model tends to overestimate the observed discharge. Despite the improvement, some differences between the two remain.

Some possible factors that can contribute to the remaining discrepancies include errors in the input data, limitations of the model structure or complexity and uncertainties in the calibration procedure itself. For a simulated model, day-to-day observations are unreliable due to uncertainties in the input data and model assumptions. Hydrological models are inherently simplified representations of complex natural systems. Therefore some level of uncertainty and discrepancy between the model outputs and observed data is expected for day-to-day discharge.

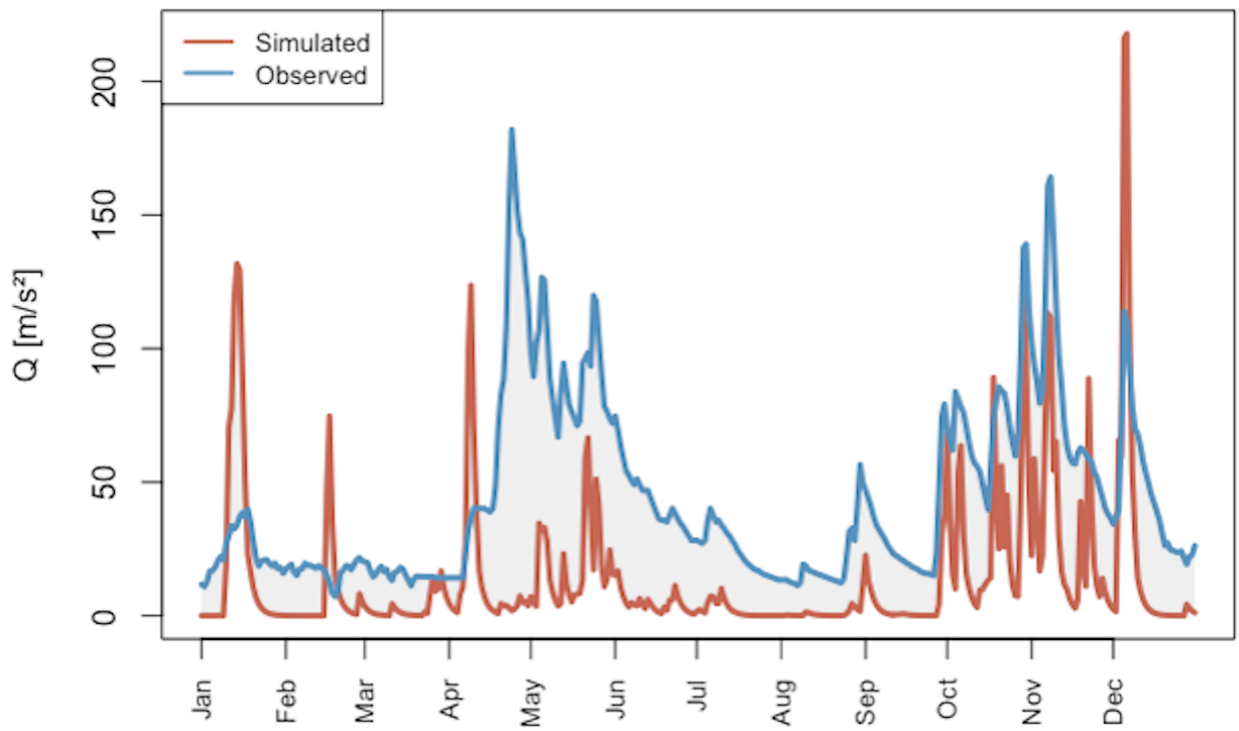


Figure 5.1: Comparison of simulated and observed daily discharge for the year 1996 before calibration. The red line represent the simulated discharge while the blue line represent the observed discharge.

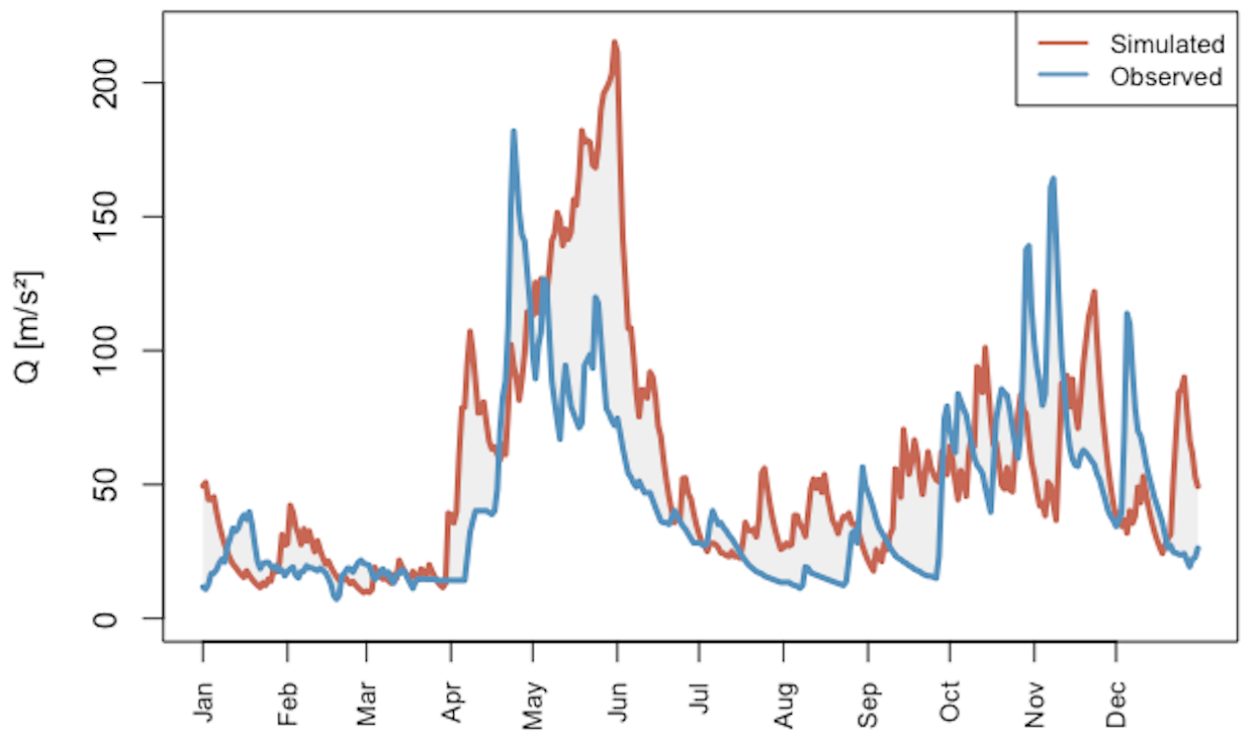


Figure 5.2: Comparison of simulated and observed daily discharge for the year 1996 after calibration. The red line represent the simulated discharge while the blue line represent the observed discharge.

The overestimation of the calibrated model is significant in May and June. The temperature (Figure 5.3), precipitation (Figure 5.4), snowpack (Figure 5.5), soil moisture (Figure 5.6), storage for upper (Figure 5.7) and lower (Figure 5.8) reservoir, actual evapotranspiration (Figure 5.9) and effective precipitation (Figure 5.10) is plotted for the year 1996 to try to understand which process is not being modeled so accurately.

In the simulated period shown in Figure 5.3 - 5.10, the month of May starts approximately on day 120. Around this time, both precipitation and effective precipitation indicate a significant amount of rainfall. According to the snowpack data, all the snow has melted by this time. As a result of increasing precipitation, the storage for the upper and lower reservoirs starts to fill up. The soil moisture also shows a slight increase during this period, which is expected, before gradually decreasing due to rising temperatures. One possible explanation for the overestimation could be the fluctuations observed in actual evapotranspiration during this time. Other than this, there is no clear explanation for this overestimation. The overestimation suggests that the model may need further refinement to predict simulated discharge better.

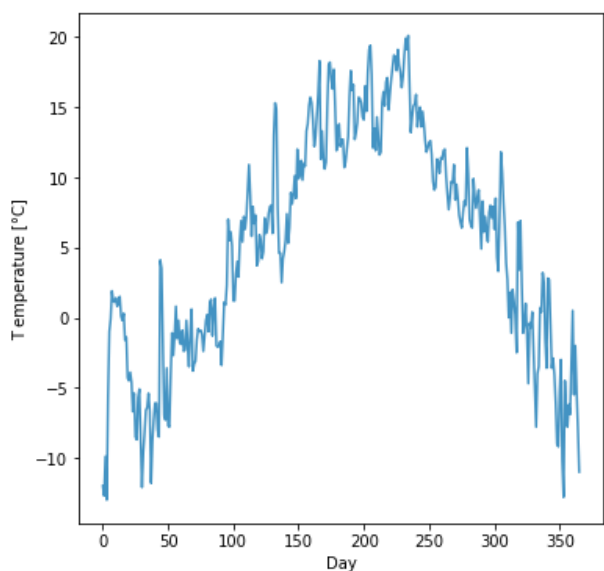


Figure 5.3: Daily temperature year 1996

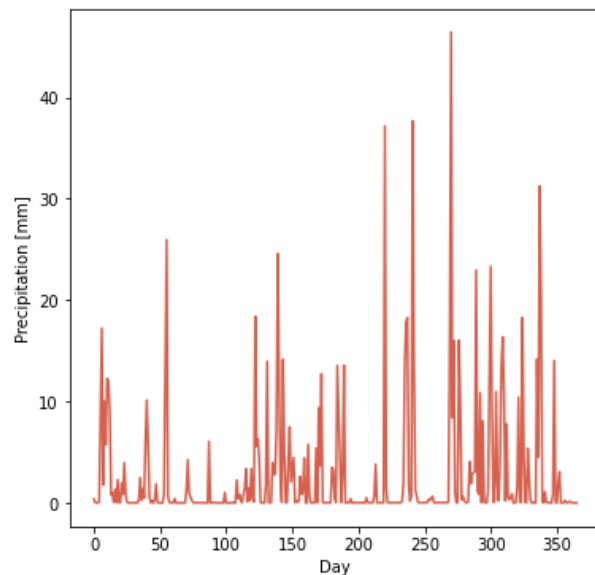


Figure 5.4: Daily precipitation year 1996

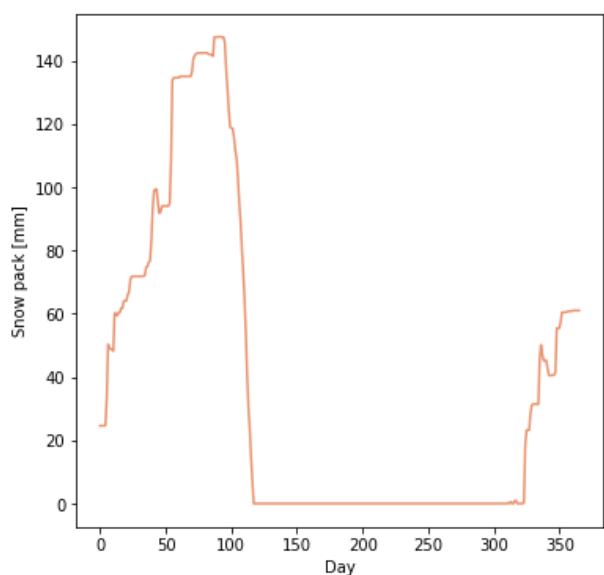


Figure 5.5: Snowpack year 1996

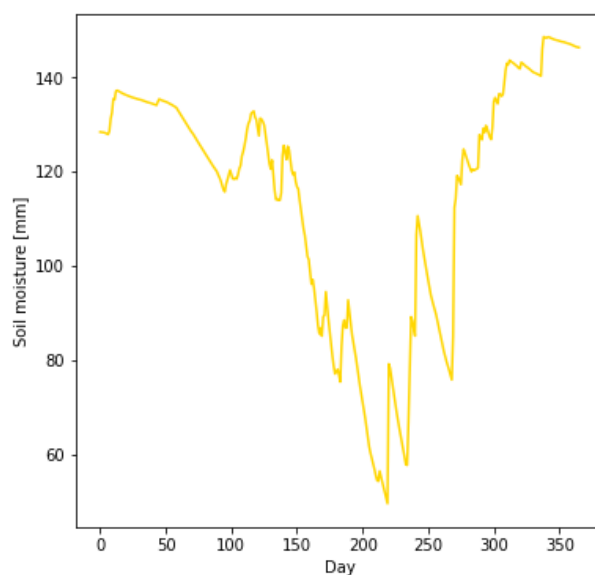


Figure 5.6: Soil moisture year 1996

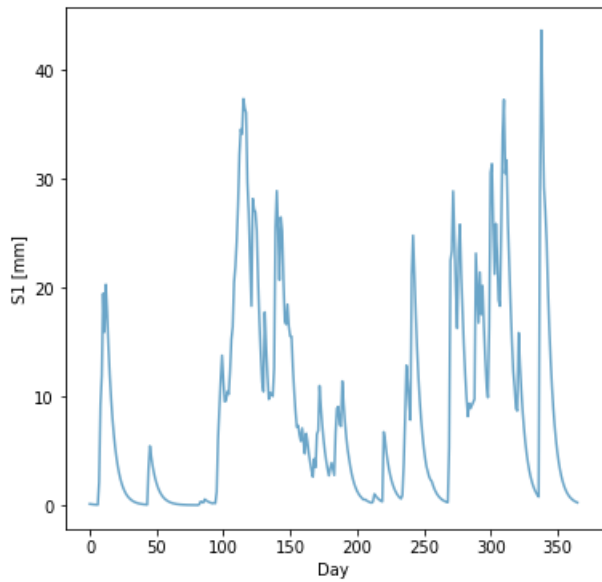


Figure 5.7: Storage upper reservoir year 1996

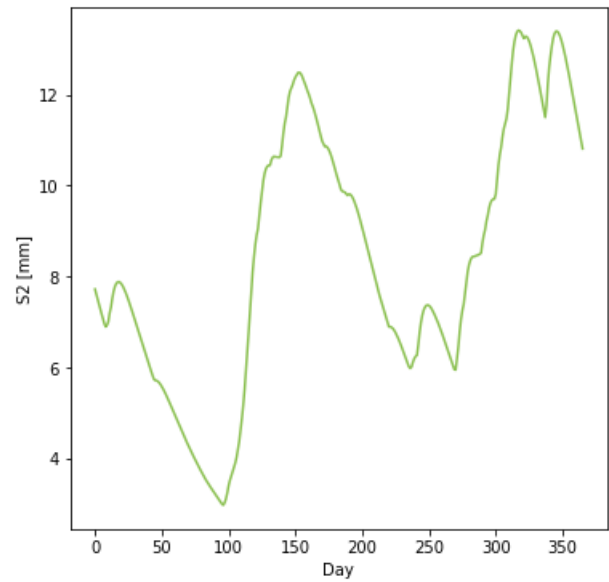


Figure 5.8: Storage lower reservoir year 1996

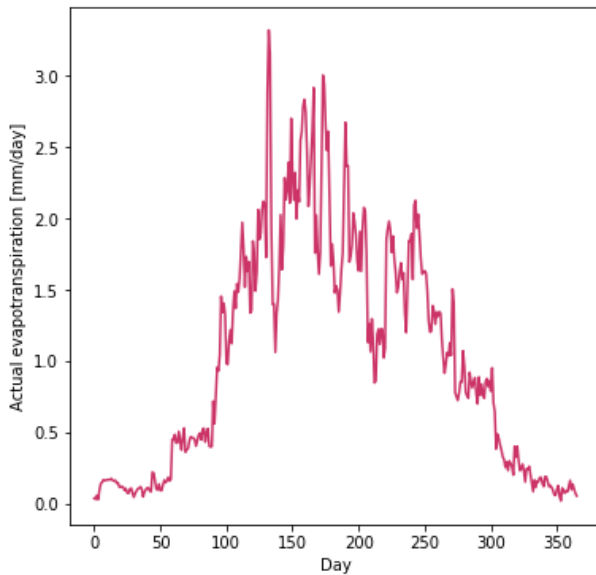


Figure 5.9: Actual evapotranspiration year 1996

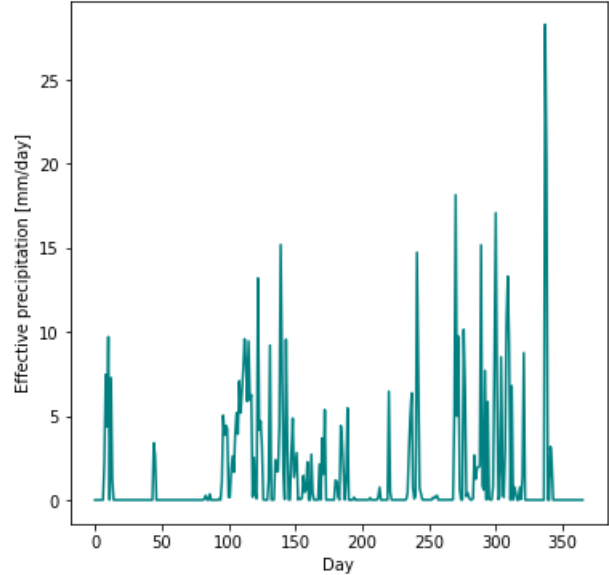


Figure 5.10: Effective precipitation year 1996

The calibration process involved running a Python script to determine the optimal parameters. Despite the overestimation, the calibration resulted in a Nash-Sutcliffe efficiency of 73.4%. According to Table 4.4, this indicates a good model performance and the calibration was deemed successful. The model was then validated using an independent dataset, resulting in a Nash-Sutcliffe efficiency of 77.7% and a Pearson correlation of 89.0%. According to Table 4.4 and Table 4.5 this indicates a very good model performance with a very high correlation. These high values suggest that the model is reliable and can accurately predict discharge values in the region. Figure 5.11 shows simulated and observed discharge for the validation period. The red line represents the simulated values, while the blue line represents the observed values. From the figure, it is evident that the model captures the trends quite well. However, the model appears to struggle to predict some high values accurately. Despite these differences, the high values of Nash-Sutcliffe efficiency and Pearson correlation indicate that the model is performing well and producing good results. This suggests that it is a reliable and accurate model. Hydrological modeling is complex, and there will always be some errors in the model predictions.

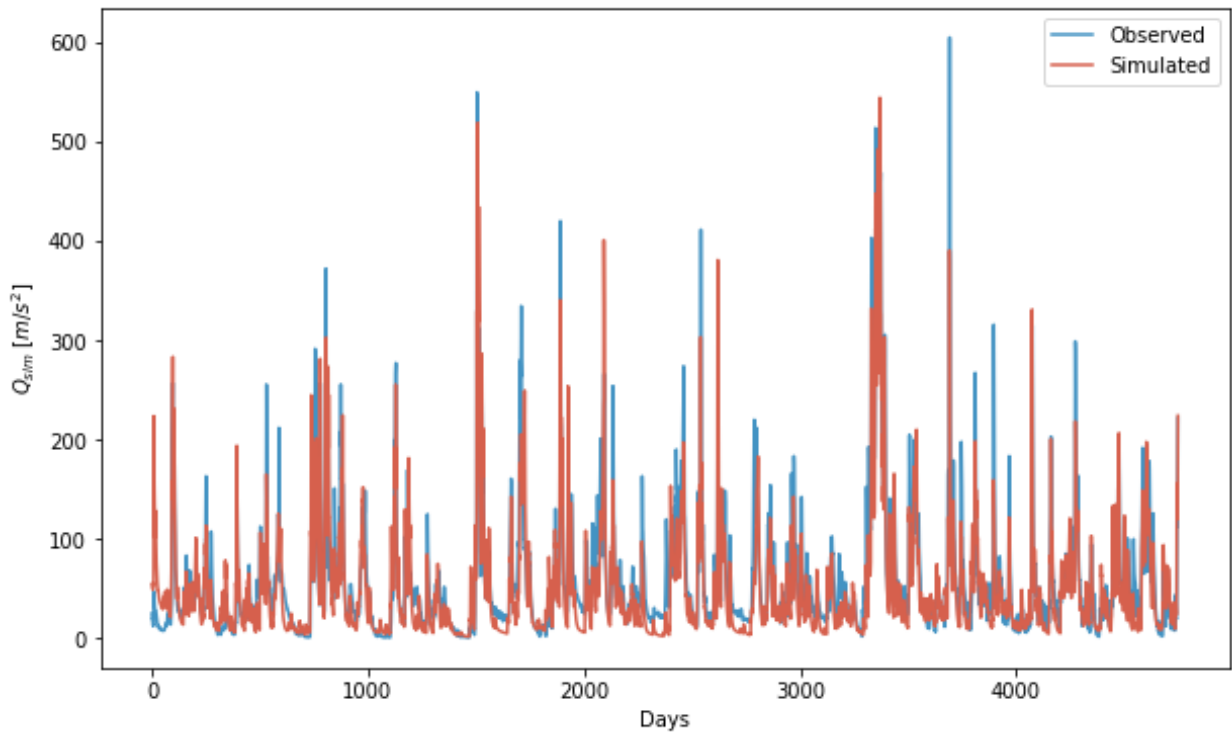


Figure 5.11: Comparison of simulated and observed daily discharge for the validation period. The red line represent the simulated discharge while the blue line represent the observed discharge.

This study's calibration and validation results are consistent with previous research on the calibration of HBV hydrological models in the area. Lawrence et al. (2009) investigated the calibration of HBV models in Norway using PEST parameter estimation. Some of the catchments investigated were nearby the Tovdal catchment. The results of their study were quite similar to those found in this study. Specifically, they found Nash-Sutcliffe values for each catchment model, calculated from daily observed versus simulated discharge. The Nash-Sutcliffe values ranged from 0.70 to 0.84 for daily values in the catchments near Tovdal. Some of the catchments achieved values of 0.85 to 0.95 for weekly values, although this study did not investigate weekly values.

A potential limitation of this study is that the Tovdal catchment is much larger than the catchments investigated by Lawrence et al. (2009) nearby Tovdal. This difference in catchment size may have an impact on the results. In Lawrence et al.'s (2009) study, the larger catchments had daily Nash-Sutcliffe values ranging from 0.85 to 0.92. This suggests that the simplified model used in this study performs worse than the "Nordic" HBV model used by Lawrence et al. (2009). This is not a surprise since the "Nordic" HBV model considers the elevation, i.e., it uses different parameters for different ranges of elevations, which gives much more flexibility to the parameters' tuning. However, the fact that the results are similar in daily values indicates that the educational version performs well, given its simplified assumptions.

Figure 5.12 shows a scatter plot where simulated and observed discharge values are plotted against each other. The black dashed line drawn in the figure is a reference line that represents an ideal relationship between the observed and simulated values. The line has a 45-degree angle and goes through the origin (0,0). This means that if the observed and simulated values were the same, all the points in the figure would lie on this line.

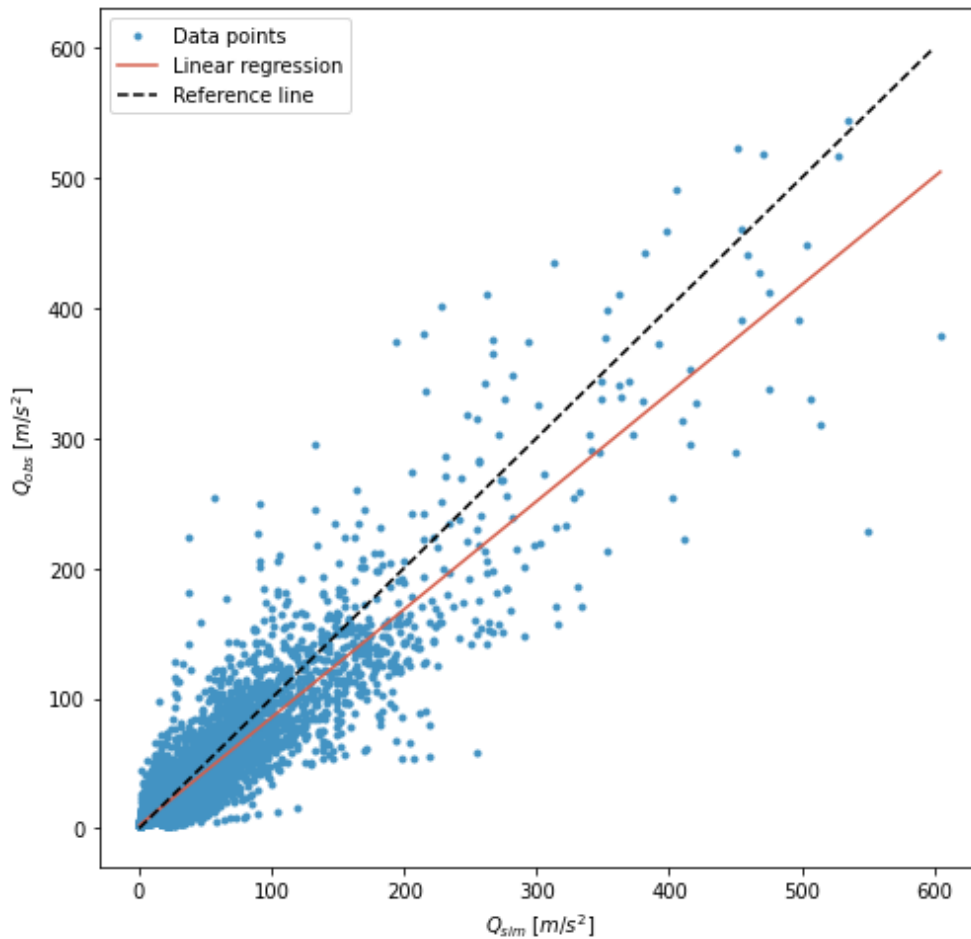


Figure 5.12: Scatter plot showing the relationship between observed and simulated discharge values, with a linear regression line (red) and a reference line (black dotted) representing an ideal relationship

The red linear regression line is often included in figures to assess how well the simulated values correspond to the observed values. The closer the red line is to the black line, the better the correspondence is between the observed and simulated values. If the points are scattered around the figure, it may indicate that the model does not accurately simulate the observed values. In this figure, the red line is below the black dashed line. This indicates that more points are below the 45-degree line, suggesting that the model overestimates the observed values. The points representing high discharge values are both above and below the black line, indicating that high values occur in both observed and simulated values. Therefore, the model does not simulate more extreme events than what has been observed.

In this case, the model tends to overestimate the observed values, which could be due to various factors, such as inadequate parameterization or input data. However, the model used in this study is an educational version with simplifications. It is possible to improve the model further, which may be necessary. The main purpose of this study is not to predict the discharge accurately, but to evaluate the change in discharge between different scenarios. Therefore, it is reasonable to expect that in all scenarios, the model will slightly overestimate the discharge. However, their difference will not have the same overestimation (since the errors will tend to cancel out). Overall, the hydrological model used in this study is considered reliable and helpful in predicting future discharge values in Agder County. The results show that the optimized parameters improved the model predictions' accuracy, providing a more reliable tool for hydrological analysis.

5.2 Optimized Parameters

The calibration script in Python (Appendix D) saves the optimized parameters in a file. These parameters are obtained through GA in the Python script. Table 5.1 presents the resulting optimized parameters and their corresponding ranges given from Table 4.2 [38]. All optimized parameter values are within their respective ranges.

Furthermore, the optimized parameters meet the requirement $PWP \leq FC$. The calibration process has successfully identified parameter values that allow the HBV model to effectively simulate the observed discharge values. These optimized parameters were then used in further simulations to investigate the impacts of climate change on hydropower potential in Agder County.

Table 5.1: Optimized parameters and their respective ranges

HBV Parameter	Optimized Value	Range Considered
T_t	1.2427	-1.0 - 2.0
DD	1.5025	1.0 - 5.0
FC	75.4551	50.0 - 500.0
BETA	1.2566	1.0 - 4.0
C	0.0796	0.01 - 0.1
K_0	0.1374	0.1 - 1.0
L	53.1932	10.0 - 100.0
K_1	0.1406	0.1 - 1.0
K_2	0.0122	0.001 - 1.0
K_{perc}	0.0236	0.001 - 1.0
PWP	67.2816	50 - 250

5.3 Temperature and Precipitation

The model takes temperature and precipitation as the main inputs. The data for these variables have been obtained from the Norwegian Centre for Climate Service, as described in Chapter 4.2.1. The figures have been generated to visualize how temperature and precipitation are expected to change over the next century. Both temperature and precipitation have a significant impact on discharge, as increased temperatures can lead to increased evaporation, while changes in precipitation patterns can result in drought periods that reduce water availability. These changes can lead to reduced power production and increased pressure on water resources. Increased precipitation can also cause flooding due to heavy rainfall, leading to infrastructure and equipment damage and reduced access to water resources.

Agder County is known for its sunny and warm climate, and it is expected to be vulnerable to the impacts of climate change. Figure 5.13 shows the temperature change in Agder County, with the median of climate models displayed and smoothed to remove short-term variability. The blue line represents the RCP4.5 scenario, while the red line represents the RCP8.5 scenario. As seen from the figure, the temperature is projected to increase throughout the upcoming century for both scenarios, with RCP8.5 showing a more significant increase. The average annual temperature is expected to be just below 10 °C by the end of the century, representing an increase of approximately 4 °C from the reference period 1971-2000. In RCP4.5, this increase is projected to be around 2.5 °C.

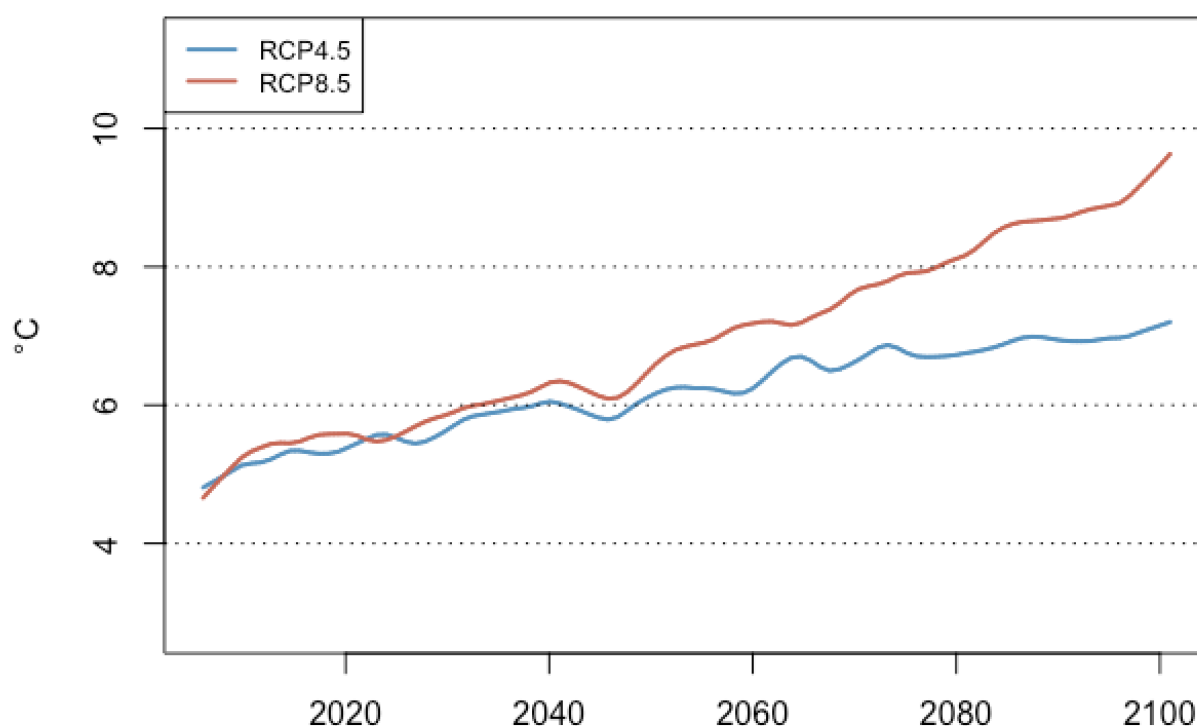


Figure 5.13: Yearly average temperature in Agder County displayed as the median of the climate models. The graphs are smoothed. The blue line represents the RCP4.5 scenario, while the red line represents the RCP8.5 scenario.

Figure 5.14 displays the projected percentage change in yearly average precipitation for the next century relative to the reference period of 1971-2000. The graph depicts the median of all models and the graphs have been smoothed to remove short-term variability. The blue line represents the RCP4.5 scenario, while the red line represents the RCP8.5 scenario. The figure suggests that, under RCP4.5, the increase in precipitation will not be significant until after 2080. From 2080, the increase will range from around 3% to slightly over 10%. Under RCP8.5, precipitation will increase until 2040 before stabilizing until around 2070. After 2070, there will be a substantial increase, with precipitation reaching almost 15% above the reference period of 1971-2000 towards the end of the century.

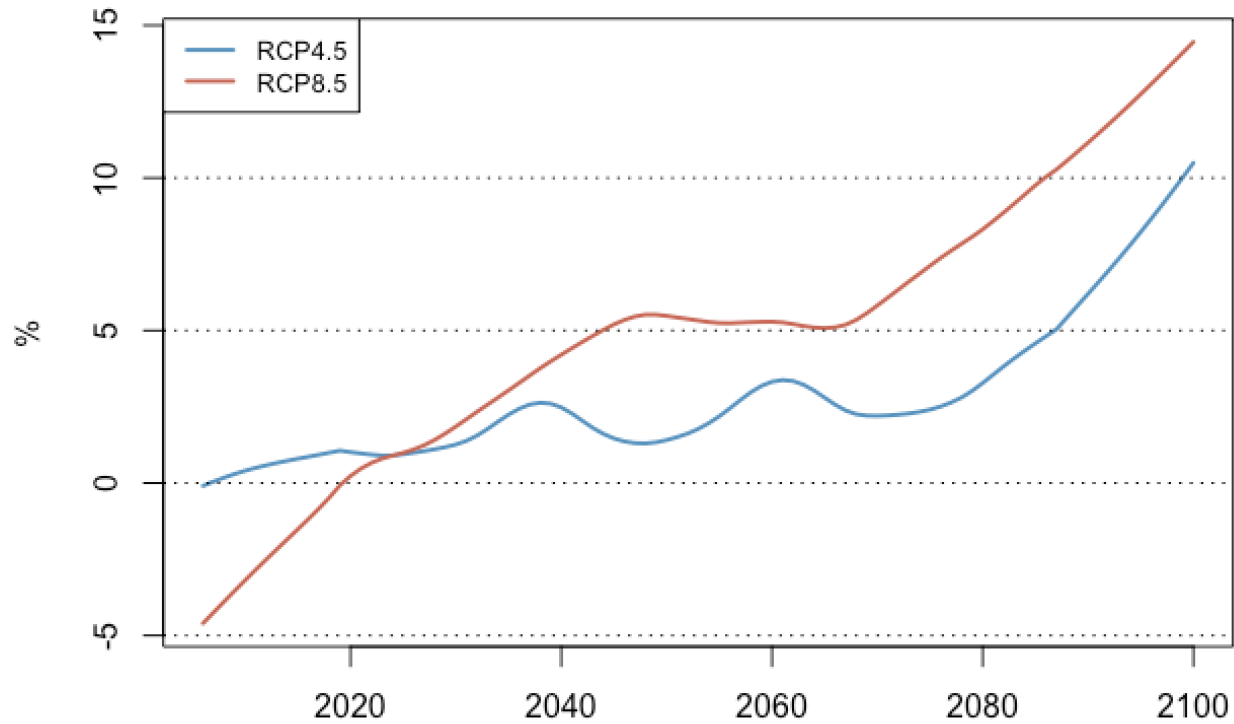


Figure 5.14: Projected percentage change in yearly average precipitation from 1971-2000 reference period for Agder County. The graphs are smoothed and shows the median of the climate models. Blue line represents RCP4.5 scenario while red line represents RCP8.5.

This study's temperature and precipitation predictions are based on simulations from different climate models, as described in Chapter 4.2.1. It is important to note that inherent uncertainty is associated with these predictions. Hydrological models are generally not reliable for day-to-day simulations. Therefore it is impossible to use temperature and precipitation data to predict the weather for a given day in the future. However, these predictions can provide valuable insights into trends and changes over a period of time.

5.4 Annual Discharge

The main output of the hydrological model is the estimated discharge for each day during the simulation period. In Figure 5.15, the total annual discharge is presented as a percentage change from the reference period 1971-2000. The lines represent the median values. The graphs are smoothed to remove short-term variability, and the shaded areas behind represent the variations among different climate models.

The graph shows that in the moderate scenario (RCP4.5), there is little change in the discharge until the end of the century. The median projection indicates an increase in annual runoff of 9% in RCP4.5. The worst-case scenario (RCP8.5) shows an increase starting around 2040, and the median projection indicates an increase of 18% by the end of the century.

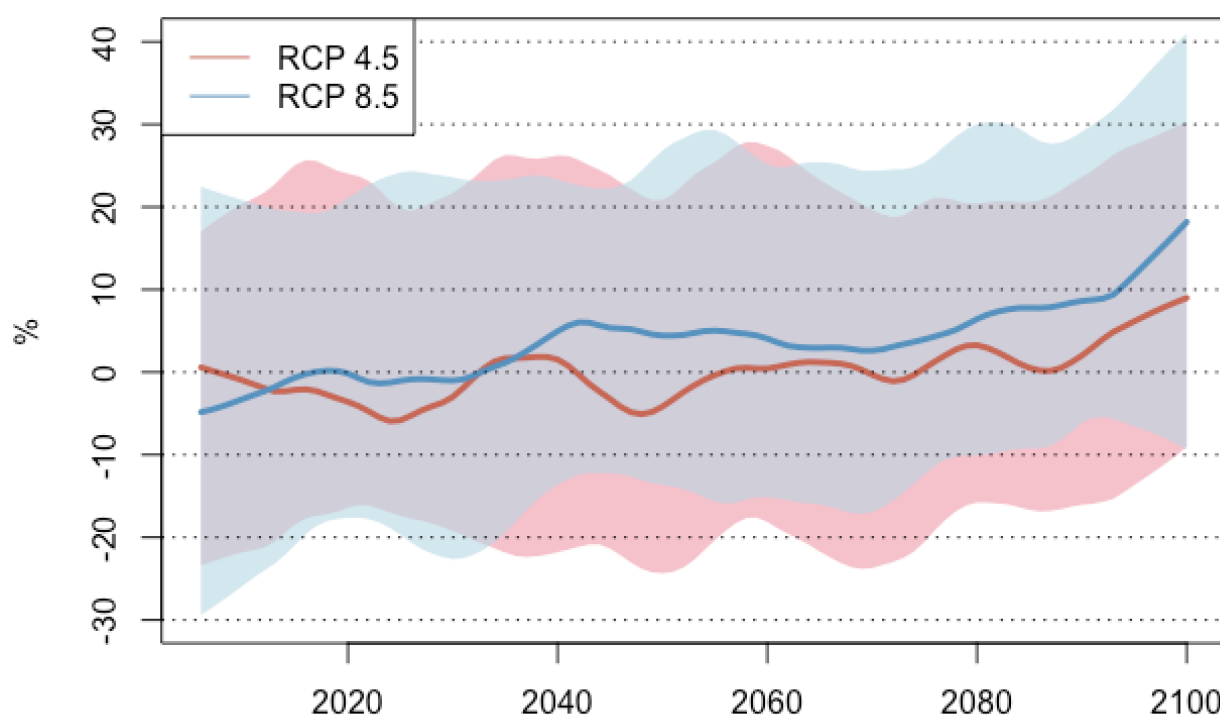


Figure 5.15: Estimated total annual discharge as a percentage change from the reference period of 1971-2000. The median of the climate models is used and smoothing is applied to the graphs to remove short-term variability. The shaded areas behind the lines represent variations among different climate models.

The uncertainty in the projections of annual discharge over the simulation period is primarily driven by the variability in the different climate models used in the study. As shown in Figure 5.15, the shaded areas behind the median lines indicate the spread of the different climate models. The larger the shaded area, the greater the spread of the climate models, increasing the uncertainty level in the projections.

To further illustrate this point, Figure 5.16 and Figure 5.17 show the different climate models used in the RCP4.5 and RCP8.5 scenarios, respectively. It can be seen that there is a wide range of projected changes in annual discharge among the different models. The spread in the model projections can be attributed to several factors, including differences in the model structure, input data and assumptions about future greenhouse gas emissions and climate change impacts.

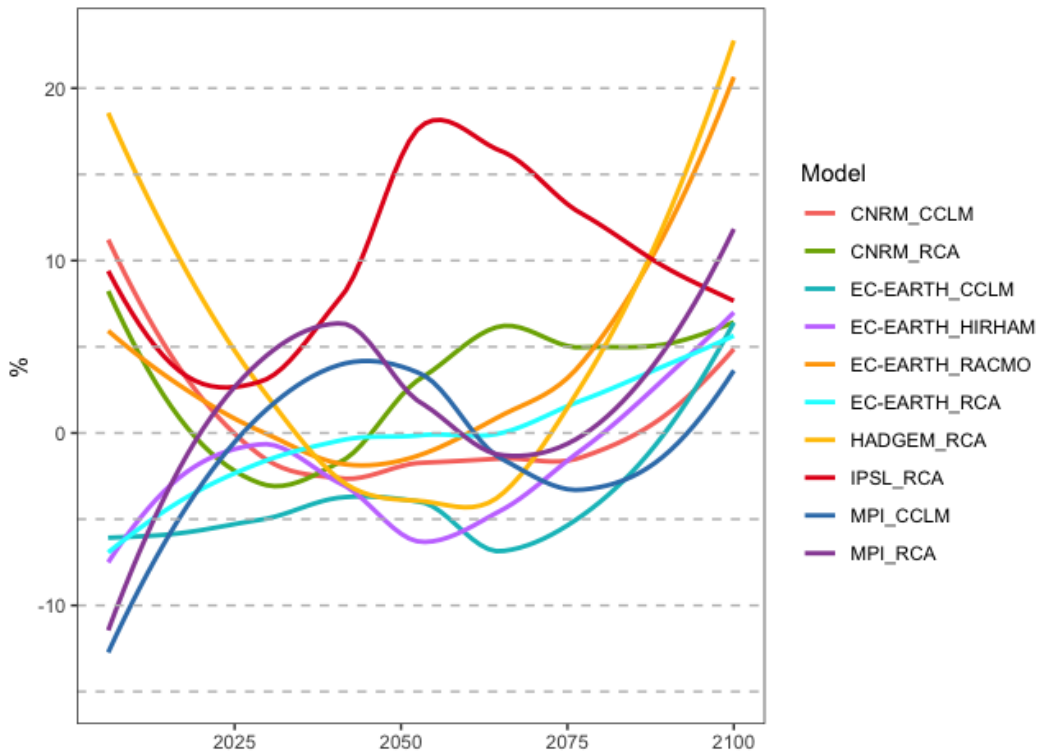


Figure 5.16: Different climate models used in the RCP4.5 scenario are shown as percentage changes from the reference period 1971-2100. The graph illustrates the wide range of projected changes in annual discharge among the different models. Smoothness is applied to remove short-term variability.

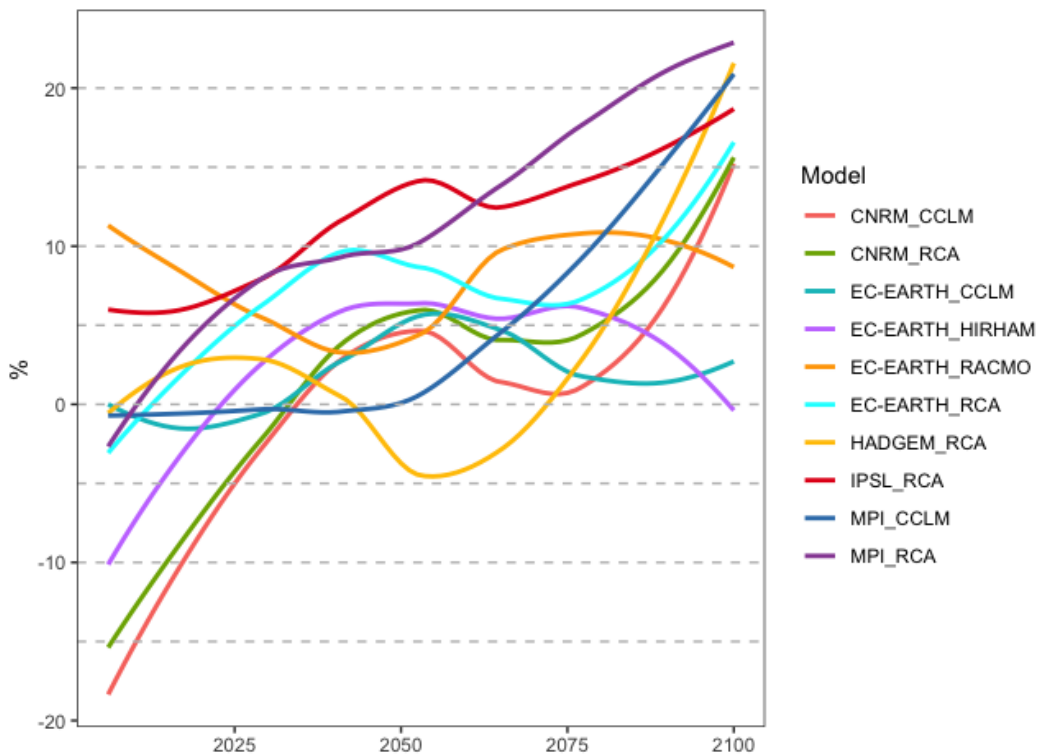


Figure 5.17: Different climate models used in the RCP8.5 scenario are shown as percentage changes from the reference period 1971-2100. The graph illustrates the wide range of projected changes in annual discharge among the different models. Smoothness is applied to remove short-term variability.

Hanssen-Bauer's et al. (2015) study projected an increase in annual discharge for Norway, with a 3% increase for RCP4.5 and a 7% increase for RCP8.5. Their study also had a large spread in the results of different climate models. [31] For the Agder region, the Norwegian Centre for Climate Services forecast said that the average annual discharge is expected to remain approximately unchanged, despite an expected increase in precipitation [32]. This is because the increased temperature will also lead to increased evapotranspiration, which offsets the effect of increased precipitation.

There are some differences between the findings of this study and those of Hanssen-Bauer et al. (2015). This study projected an increase in discharge of 9% (RCP4.5) and 18% (RCP8.5). When looking more closely at the changes in temperature and precipitation, it is expected that Agder County will have a lower temperature increase than the rest of Norway, with an increase of 2.4 °C for Agder County compared to 2.7 °C for Norway (RCP4.5) and 3.9 °C for Agder County compared to 4.5 °C for Norway (RCP8.5). This should result in a smaller increase in evapotranspiration and therefore a greater change in discharge for Agder County. The expected increase in precipitation for Agder County is 10% compared to 8% for Norway (RCP4.5), and 15% for Agder County and 18% for Norway (RCP8.5). With a lower temperature increase and higher precipitation increase for the RCP4.5 scenario, it is reasonable to assume that the discharge will increase, as this study shows. For the RCP8.5 scenario, temperature and precipitation are expected to be lower for Agder County than for Norway. However, with a smaller increase in temperature, there will be less evapotranspiration and more of the rain will become discharge. This could be one explanation for why the results of this study differ from those of Hanssen-Bauer et al. (2015) and the forecasts for the Agder region by the Norwegian Centre for Climate Services. [31]

The study conducted by Koestler et al. (2019) on inflow to Norwegian hydropower plants found that, under the RCP8.5 emission scenario, inflow is expected to increase by around 7% by the end of the century for Norway, with a greater increase of over 10% in the southern part of the country. [33] These results are more consistent with the findings of this study.

5.5 Monthly Discharge

The projected changes in monthly discharge are expected to be considerably larger than for annual discharge due to the combined effect of changes in temperature and precipitation. Warmer temperatures result in increased evaporation rates, which can cause a reduction in discharge during drier months. Conversely, higher precipitation levels can lead to increased discharge during wetter months and changes in snow and snowmelt regimes. These changes in temperature and precipitation can have a more significant impact on monthly discharge than on annual discharge, as they are more pronounced during certain months of the year.

Figure 5.18 shows the monthly discharge for the mid-century period, with blue and red bars representing the RCP4.5 and RCP8.5 scenarios, respectively. The percentages indicate the change compared to the reference period of 1971-2000. Figure 5.19 shows the same data for the late-century period. Both figures show that the most remarkable changes in monthly discharge occur during winter (November through April). Winter months will experience significantly greater discharge, while summer months (May through October) will experience reduced discharge, resulting in negative percentage changes. During the mid and late centuries, there will be less discharge in the summer and more in winter. Figure 5.18 indicates that the largest differences between the RCP4.5 and RCP8.5 scenarios occur during the winter, with more minor differences during the summer months. Figure 5.19 shows similar trends, but with higher percentage changes.

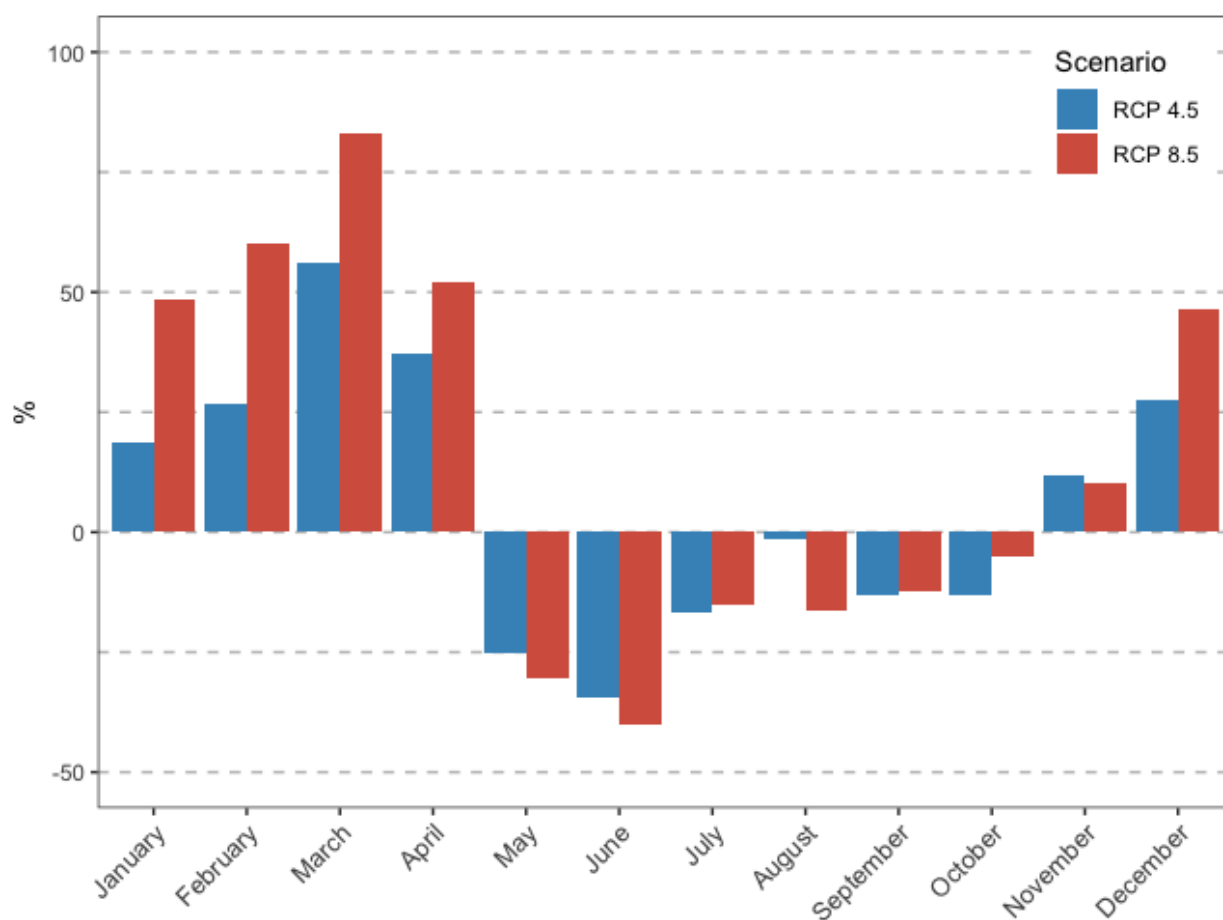


Figure 5.18: Monthly discharge changes from the reference period (1971-2000) for the mid-century period (2036-2065) under the RCP4.5 and RCP8.5 scenarios. The median of the climate models is used.

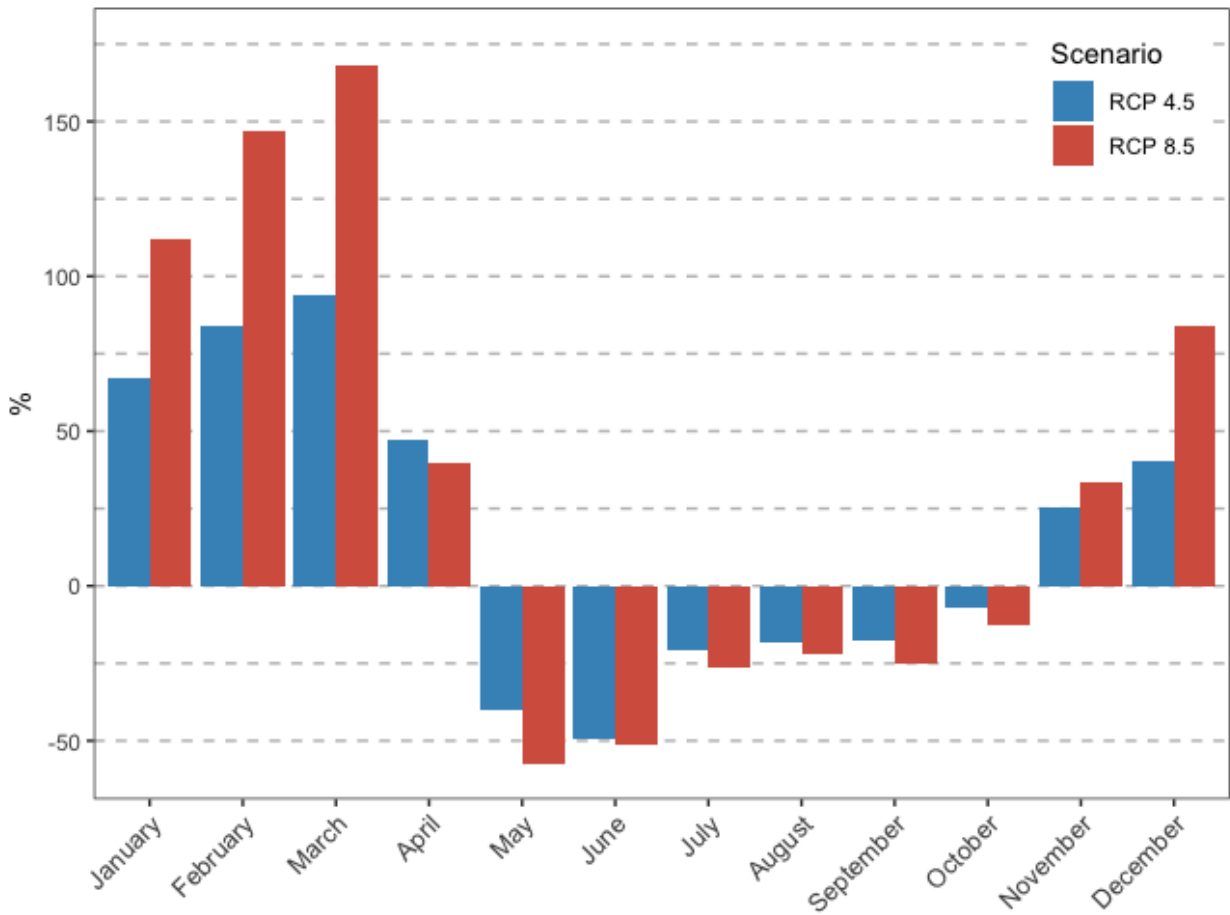


Figure 5.19: Monthly discharge changes from the reference period (1971-2000) for the late-century period (2071-2100) under the RCP4.5 and RCP8.5 scenarios. The median of the climate models is used.

The big changes in winter are primarily due to increased precipitation and a shift from snow to rain as temperatures rise. This leads to increased water flowing into rivers and lakes, resulting in higher winter discharge. On the other hand, the big changes in summer months are due to earlier snowmelt caused by rising temperatures and higher evaporation losses due to increased temperatures. This leads to a decrease in the amount of water stored in snow and ice during winter, leading to lower summer discharge. Therefore, the effects of climate change on temperature and precipitation patterns significantly impact the seasonal changes in discharge. This higher variability between seasons is a challenge for hydropower production. On one hand the hydropower potential increases, on the other it is more variable across the year, which makes its exploitation more demanding.

To compare the changes from mid- to late-century, Figure 5.20 and Figure 5.21 are plotted. Figure 5.18 shows the monthly discharge for RCP4.5 for mid- and late-century. Mid-century (2036-2065) is represented by the blue line, and the red line represents late-century (2071-2100). Figure 5.19 shows the monthly discharge for RCP8.5 for mid- and late-century, with the same color scheme and percentage change reference period. In Figure 5.20, which corresponds to emission scenario 4.5, the most significant difference between the two periods is observed from January to April. This indicates that the increase in discharge will be greater during these months over the century. There are more minor differences throughout the rest of the year, which means that the changes in these early months significantly contribute to the increase in annual discharge over the century. These trends are even more visible in Figure 5.21, representing emission scenario 8.5.

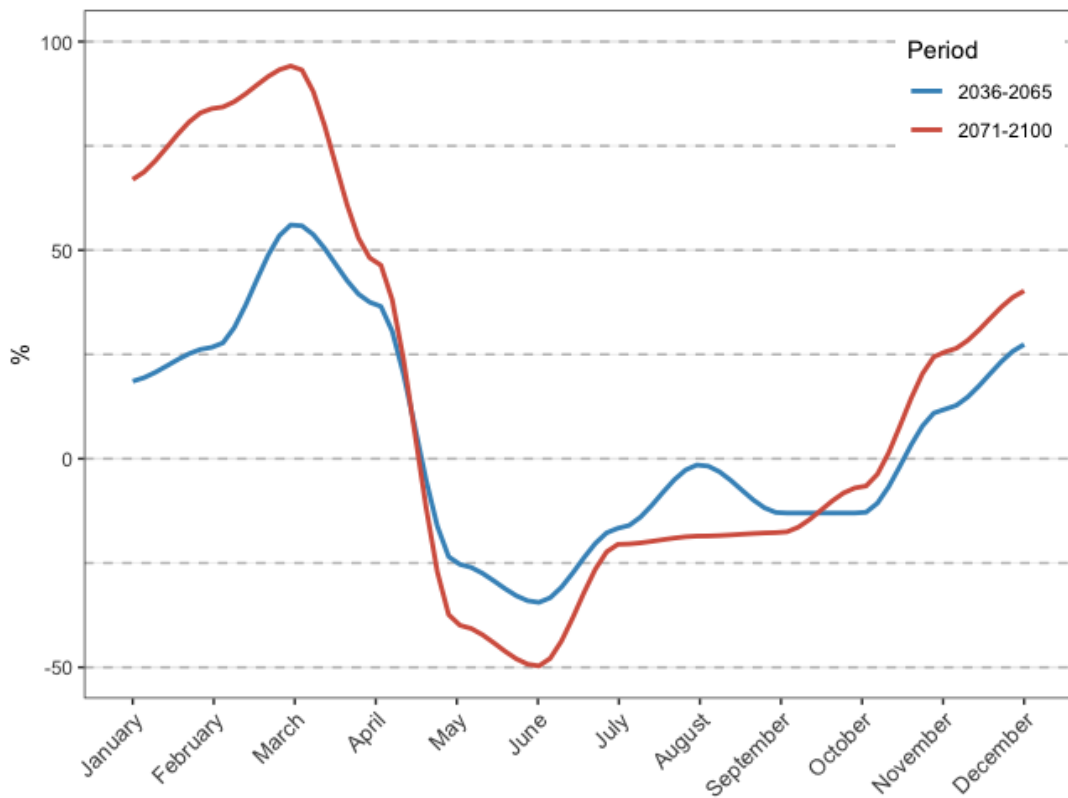


Figure 5.20: Monthly discharge for RCP4.5 for mid and late-century. The blue line represents the mid-century, and the red line represents the late-century. The graphs show the percentage change from the reference period 1971-2000. The median of the climate models is used, and smoothing is applied to the graphs to remove short-term variability.

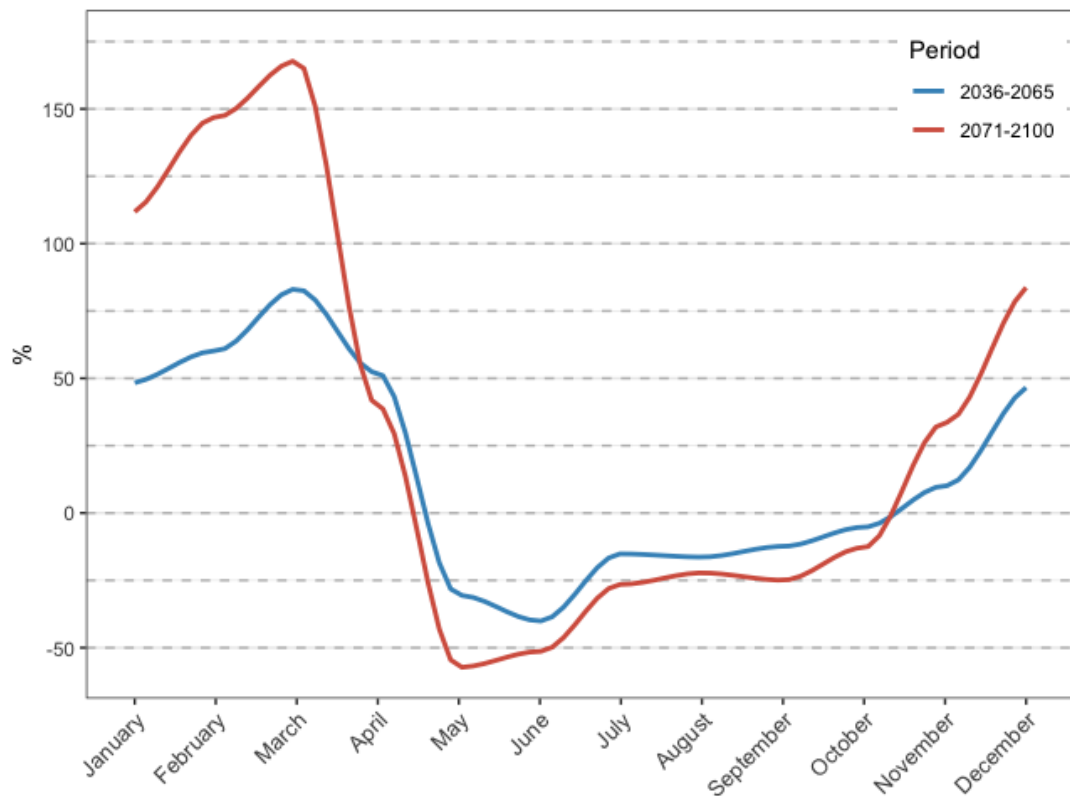


Figure 5.21: Monthly discharge for RCP8.5 for mid and late-century. The blue line represents the mid-century, and the red line represents the late-century. The graphs show the percentage change from the reference period 1971-2000. The median of the climate models is used, and smoothing is applied to the graphs to remove short-term variability.

In Roald et al.'s (2006) study, the results showed moderate changes in annual streamflow, but more significant alterations in the seasonal distribution of streamflow. In the winter season, the study projected an increase in streamflow, like this study. However, during spring, they found a moderate decrease in streamflow in the southern regions of Norway. This study predicts an increase in March and April, while a decrease in May. Furthermore, both studies indicated a decrease in streamflow during the summer season. In the autumn, the moderate scenario by Roald et al. (2006) predicted an increase in streamflow, while the extreme scenario suggested a decrease in low-lying basins in the country's southern parts. In this study, there is a decrease in September and October, while an increase in November for both scenarios. The results of Roald et al.'s (2006) study and the findings presented in this study are therefore consistent in some aspects but differ in others. Both studies identified an increase in winter streamflow, indicating a potential response to climate change. This suggests a common understanding that winter discharge may become more pronounced in the future. Both studies align in projecting a decrease in discharge during the summer, indicating a potential water resource challenge.

The increasing discharge during the early months of the year indicates that winters in Agder County are becoming warmer and wetter, leading to less snow accumulation. This can be attributed to rising temperatures in the region, as well as an increase in precipitation. With temperatures no longer below freezing, snow will not accumulate, and most precipitation will occur as rain instead. As the level of discharge increases, it can cause flooding, erosion and sediment transport, which can impact the ecosystem, water quality and infrastructure. Changes in the timing and magnitude of discharge can also impact hydropower generation and water availability for irrigation and other uses. Good river and waterway management strategies may be required to mitigate the potential negative consequences of increased discharge. This can include measures such as reservoir expansion, expansions of waterways and floodplain zoning to accommodate higher water volumes during extreme rainfall events.

During the summer months, it is crucial for Agder County to have sufficient water stored in reservoirs to meet the power demand. The summers are expected to become increasingly dry, which amplifies the need for greater capacity in the reservoirs. Without this, Agder County will become even more reliant on importing electricity from abroad, resulting in higher electricity prices. However, the increasing winter discharge also presents opportunities for hydropower in Agder County. By optimizing existing power plants, considering expansions of waterways and aggregates, as well as enhancing generator performance, it is possible to achieve increased production and better utilization of the increasing winter discharge. This can result in sufficient reservoir storage to meet the year-round demand.

5.6 Using the HBV Educational Version for Hydrological Modeling

The educational version of the HBV model has been successfully used as a hydrological model to assess the impact of climate change on potential hydropower in Agder County. Despite its simplified assumptions, the calibration process improved the model's performance in predicting discharge values, resulting in a good Nash-Sutcliffe efficiency and Pearson correlation. The calibration of hydrological models can be challenging, as it requires balancing the need for accurate predictions with a model that is simple enough. However, the results of this study indicate that the simplified educational version of the HBV model used was able to produce reasonably accurate results, despite its simplifications. The Nash-Sutcliffe efficiency values obtained in this study were similar to those obtained by Lawrence et al. (2009) for daily values in the same area as the Tovdal catchment, indicating that the model's simplicity does not surpass its accuracy. These findings demonstrate the potential of the HBV educational version as a valuable tool for teaching and learning hydrological modeling concepts in a simplified and accessible way.

The HBV educational version was initially available in Excel spreadsheet and MATLAB code, but has now been translated to Python, making it more accessible to a broader audience. The Python code's simplicity, ease of use, and relatively short simulation times make it a valuable tool for hydrological modeling. It is important to note that users should have some prior knowledge of hydrology and relevant processes to use the model effectively.

5.7 Uncertainties

Uncertainty is a central concept in hydrological modeling, as it relates to the degree of confidence that can be placed in the results of a model.

One source of uncertainty in this study is related to using an educational version of the HBV model, which has simplified components compared to the full version. This may have led to an insecurity of the variability of the simulated hydrological variables, such as discharge and evapotranspiration. Additionally, the simplified model components may affect the calibration of the model, which could lead to biased results. Parameter uncertainty is a significant source of uncertainty in the calibration process of hydrological models. The calibrated parameters are only estimates of the actual values, and there is always some uncertainty associated with them.

Parameter uncertainty can arise from various sources, including errors in measurement, incomplete understanding of the hydrological processes and inadequacy of the model structure. For example, different combinations of parameters can produce equally good model fits, making it challenging to determine the optimal set of parameters. Furthermore, the selection of parameter values can be influenced by the range and distribution of the observed data used in the calibration process. Sensitivity analysis can also be performed to assess the impact of each parameter on the model output and identify the most influential ones. This is not done in this study.

There are also uncertainties related to future greenhouse gas emissions and the resulting climate scenarios. The RCP4.5 and RCP8.5 scenarios used in this study are based on assumptions about future emissions, which are subject to uncertainties related to economic, technological and societal developments. Moreover, the global climate system is complex and involves many feedback mechanisms, which can amplify or dampen the effects of greenhouse gas emissions. As a result, uncertainty in the magnitude and timing of future climate changes can affect the simulation results.

5.8 Limitations Related to the Datasets

The quality and reliability of the data used in a study can significantly impact the accuracy and validity of its findings. Further, the limitations related to the datasets used in this study and their impact are discussed.

The dataset used for temperature and precipitation in this study is simulated values provided by the Norwegian Centre for Climate Service in collaboration with NVE. Due to model simplifications and insufficient knowledge of the physical processes in the earth system, the model results may not correspond perfectly with observed values. Hanssen-Bauer et al. (2015) acknowledged uncertainties associated with climate projections, including future anthropogenic emissions, natural climate variations and climate models. Uncertainties related to future anthropogenic emissions stem from various factors such as economics, population growth, and energy sources, which are driven by political decisions. Although emission scenarios such as RCP4.5 and RCP8.5 are widely accepted and used in scientific reports, there are still significant uncertainties related to the possible outcomes. Uncertainties related to natural climate variations are largely simulated by climate models, and the use of multiple models provides an estimate of the uncertainty. Model uncertainty is also due to limitations in understanding the climate system and the limited ability to implement this understanding in a numerical mathematical framework. [31] When using the dataset of the results of Hanssen-Bauer et al. (2015), these uncertainties propagate to the present study.

For the observed temperature, some data were missing in the dataset. These missing temperature data were obtained through interpolation, which is a commonly used method for estimating temperatures at locations where no measurements have been taken. Only nine days were missing from January 1971 to December 2005. It is therefore assumed that this has little impact on the results.

For observed precipitation data, the Thiessen Polygon Method was used for four stations nearby the catchment. This is widely used to estimate the amount of precipitation in a given area. This method has limitations, as it assumes that the amount of precipitation within a polygon is uniform. However, this should not significantly impact the results, as the measuring stations are relatively close and should measure precipitation in similar amounts over a given period.

5.9 Strengths and Weaknesses

To provide a comprehensive evaluation of the findings, the strengths and weaknesses of the study are evaluated in the further.

A strength of the study is the use of parameter optimization based on GA optimization. This technique has not been used in the original educational version of HBV, making this study unique. This optimization can improve the accuracy of hydrological modeling by optimizing model parameters to fit observed data. By using this, the study improved the calibration of the model, resulting in more accurate simulations of the hydrological system in Agder County. GA optimization also enhances the credibility of the study results, as it provides a more precise approach to parameter estimation. By optimizing the model parameters based on GA optimization, the study was able to reduce uncertainty and increase confidence in the simulation results. This study also employed parameter ranges provided by Lawrence et al. (2009) to mitigate uncertainty and enhance confidence in the obtained results. By incorporating these parameter ranges, the potential variability in the outcomes was reduced and improved the reliability of the findings.

A weakness of the study is the data for long-term mean monthly potential evapotranspiration, which was not adjusted during the simulation period from 2006 to 2100. The data used for long-term mean monthly potential evapotranspiration in this study were derived from the mean evaporation from January 1971 to December 2005. However, the mean monthly potential evapotranspiration is expected to change over time, as long-term temperatures primarily influence it. Therefore, using this data set is considered a limitation of the study.

This limitation could affect the results' accuracy since evapotranspiration plays a crucial role in the water balance of a hydrological system. However, the adjusted evapotranspiration is calculated from Equation 4.7, meaning that adjustments are made based on daily temperatures during simulation. Therefore, the impact of the limitation on the accuracy of the results may be mitigated.

5.10 Contribution to the Literature

This study examines the impact of climate change on the potential hydropower in Agder County, Norway. Similar studies have been conducted in the past, but several aspects differentiate this study from others in the field. As for how this study contributes to the literature, it may provide new insights and data on the specific impacts of climate change on hydropower potential in Agder County, which could be useful for policymakers in the region. Additionally, the methodology and approach used in this study may interest other researchers studying climate change's impacts on potential hydropower in other regions.

This study uses an educational version of the HBV model, which to the author's knowledge, has yet to be utilized in previous research in Norway. While this version has some limitations and simplifications compared to the more advanced versions, the results of this study show that it can still provide valuable insights into the potential hydropower in the region. The HBV educational version has been translated to Python, which makes it accessible to a broader audience who prefer Python as an open-source programming tool. The scripts provide a straightforward and not time-consuming approach. There is important that the users of the scripts have some prior knowledge of hydrology and relevant processes to use the model effectively. The results of this study demonstrate that the educational version of HBV is a valuable tool for hydrological modeling in a simplified and accessible way.

GA parameter estimation was used during the calibration to estimate the optimal model parameters. GA parameter estimation can increase the credibility and reliability of the results by minimizing the difference between simulated and observed values. This allows for more confident conclusions to be drawn from the results of the study. The educational version of HBV did not use this approach in the Excel spreadsheet or MATLAB script.

Tovdalsvassdraget was granted protected status in 1986 and therefore, hydrological data can be studied without hydropower regulation. The Tovdal catchment spans a long distance from the northernmost region of the county to the south, making this catchment representative of Agder County. This catchment is not found used in similar studies in the field.

Chapter 6

Conclusions

Climate change has become a topic of increasing concern in recent years. Norway is one of the most hydro-dependent nations in the world. This dependency raises a question about climate change impact on future hydropower production. The specific effects of climate change on hydropower potential vary across regions, and it is crucial to understand the risks and opportunities associated with this renewable energy source. This thesis aims to assess how climate change will affect hydropower potential in Agder County over the next century.

To address this research question, an educational version of the HBV model was utilized, using future weather data from global and regional climate models under different emission scenarios as input. The model's effectiveness and capability to address the research question were also evaluated. As a result of the research question, the following conclusions can be drawn:

- The results of the study indicate that the educational version of the HBV model, despite its simplified assumptions, exhibited good overall performance. After calibration, the model tended to overestimate simulated discharge values but achieved a Nash-Sutcliffe efficiency of 73.4%. The validation phase further demonstrated the model's reliability, with a Nash-Sutcliffe efficiency of 77.7% and a high Pearson correlation of 89.0%. These findings highlight the potential of the educational version of the HBV model as a valuable tool for assessing hydropower potential and that the model's simplicity does not surpass its accuracy.
- Regarding annual discharge, the study found that the RCP4.5 scenario predicts a relatively small change throughout the century, with an increase of 9% by the end of the century. The RCP8.5 scenario projects a more substantial increase, starting around 2040 and reaching 18% by the end of the century.
- Examining the monthly discharge patterns, it becomes evident that the most significant changes occur during the winter (November to April). Winter experiences a notable increase in discharge, while the summer months (May to October) exhibit reduced discharge. The disparities between the RCP4.5 and RCP8.5 scenarios are particularly pronounced during winter, primarily driven by increased precipitation and a shift from snow to rain as temperatures rise. Notably, the early months from January to April show the most significant difference between the mid- and late-century, suggesting a greater increase in discharge during these months over the century. This indicates that winters in Agder County are becoming warmer and wetter, resulting in reduced snow accumulation.

The observed trends in future discharge patterns pose both challenges and opportunities for hydropower production in Agder County. During periods of reduced discharge, the county's reservoirs must have the capacity to store water from periods of increased discharge to meet

the power demand. If not, Agder County will be more dependent on the import of electricity from abroad, affecting electricity prices. Additionally, the increasing discharge in winter necessitates additional capacity in rivers and waterways to accommodate the higher discharge. This increasing discharge during winter can present opportunities for hydropower production in the future. By optimizing existing power plants, consider expansions of waterways and aggregates, as well as increased generator performance, it will be achieved increased production and better utilization of the increasing winter discharge.

Chapter 7

Further Work

While this study has provided valuable insights into the ease of use of the educational version of the HBV model and climate change impacts on the hydropower potential in Agder County, it would be worthwhile to investigate the following:

- To enhance the results, future studies should incorporate varying datasets for long-term mean monthly potential evapotranspiration from the simulation period; one for climate scenario RCP4.5 and one for RCP8.5. These datasets would be based on simulations, but this would provide a more realistic representation of evaporation processes and potentially improve the accuracy of the model's outcomes.
- Conducting a sensitivity analysis would be beneficial to assess the model's sensitivity to different parameters. A deeper understanding of the model's behavior and identifying the most influential factors would be gained by systematically varying the parameters and evaluating the corresponding changes in the model's output.
- This study only investigates the Tovdal catchment. Further research could explore the model's performance in different catchments beyond Agder County. Investigating if similar results are obtained in other regions or areas with different hydrological characteristics and climate conditions would contribute to a more comprehensive understanding of the model's capabilities and limitations.
- In order to address the uncertainty associated with climate change, it would be interesting to investigate additional climate scenarios such as RCP2.6 and RCP6.0.
- The results of this study have indicated that changing discharge patterns highlight the challenges associated with small waterways, it is evident that in the future, expanding these waterways and increased generator performance will become necessary. This could lead to the development of larger hydropower plants, where more of the discharge can be channeled through the hydropower plant, generating electricity instead of being bypassed during periods of high discharge. As further work, it would be interesting to conduct a cost-benefit analysis to assess the economic feasibility of expanding the waterways and enhancing generator performance.

Appendix A

Climate Models

Table A.1: Overview of GCM/RCM combinations used from EURO-CORDEX [43]

Global climate model	Ensemble member	Regional climate model	Time period	Institution
CNRM-CERFACS-CM5	r1i1p1	CCLM4-8-17	1971-2100	Climate Limited-area Modelling Community
CNRM-CERFACS-CM5	r1i1p1	RCA4	1971-2100	Swedish Meteorological and Hydrological Institute
ICHEC-EC-EARTH	r12i1p1	CCLM4-8-17	1971-2100	Climate Limited-area Modelling Community
ICHEC-EC-EARTH	r3i1p1	HIRHAM5	1971-2100	Danish Meteorological Institute
ICHEC-EC-EARTH	r1i1p1	RACMO22E	1971-2100	Royal Netherlands Meteorological Institute
ICHEC-EC-EARTH	r12i1p1	RCA4	1971-2100	Swedish Meteorological and Hydrological Institute
MOHC-HadGEM2-ES	r12i1p1	RCA4	1971-2100	Swedish Meteorological and Hydrological Institute
IPSL-CM5A-MR	r1i1p1	RCA4	1971-2100	Swedish Meteorological and Hydrological Institute
MPI-ESM-LR	r1i1p1	CCLM4-8-17	1971-2100	Climate Limited-area Modelling Community
MPI-ESM-LR	r1i1p1	RCA4	1971-2100	Swedish Meteorological and Hydrological Institute

Appendix B

Extracting Data - Python Script

This code extracts the data from netCDF files for the catchment and converts it to an Excel file.

```
from netCDF4 import Dataset
import numpy as np
import pandas as pd
import datetime

path_main_folder=(r'/Volumes/LaCie/Master_thisis/DataV1/KSSData/') #change path to folder
min_lon = 8.09
max_lon = 8.4
min_lat = 58.3
max_lat = 59.15

scenario = 'hist'
#scenario = 'rcp45'
#scenario = 'rcp85'

if scenario == 'hist':
    start_year = 1971
    end_year = 2005
else:
    start_year = 2006
    end_year = 2100

MODELS=['CNRM_CCLM'] #Change climate model here
        #['CNRM_CCLM', 'CNRM_RCA', 'EC-EARTH_CCLM', 'EC-EARTH_HIRHAM', 'EC-EARTH_RACMO',
        #'EC-EARTH_RCA', 'HADGEM_RCA', 'IPSL_RCA', 'MPI_CCLM', 'MPI_RCA']

for model in MODELS:
    precip_folder = model+'_RR_DAY'
    temp_folder = model+'_TM_DAY'

    xls_data=pd.DataFrame(columns=['Date','Month ID','Temp. (C)','Preci. (mm)'])

    for year in range(start_year,end_year+1):
        filename_precip = scenario + '_' + model + '_RR_daily_mm_' + str(year) + '.nc'
        data_precip = Dataset(path_main_folder + '//' + precip_folder + '//' + filename_precip)
        filename_temp = scenario + '_' + model + '_TM_daily_K_' + str(year) + '.nc'
        data_temp = Dataset(path_main_folder + '//' + temp_folder + '//' + filename_temp)

        time = np.array(data_precip.variables['time'][:])
        date=datetime.datetime(year,1,1)

        long = np.array(data_precip.variables['lon'][:])
        lat = np.array(data_precip.variables['lat'][:])

    ##### Comment in the right scenario

# HISTORICAL
    for i in range(len(time)):
        precip = np.array(data_precip.variables['precipitation__map_hist_daily'][i,:])*1
        precip = np.where(precip<=3000., precip, np.nan)
```

```

precip = np.where(long>=min_lon, precip, np.nan)
precip = np.where(long<=max_lon, precip, np.nan)
precip = np.where(lat>=min_lat, precip, np.nan)
precip = np.where(lat<=max_lat, precip, np.nan)
precipitation_avg = np.mean(precip[~np.isnan(precip)])

temp = np.array(data_temp.variables['air_temperature__map_hist_daily'][i,:])*1-273.15
temp = np.where(temp<=3000., temp, np.nan)
temp = np.where(long>=min_lon, temp, np.nan)
temp = np.where(long<=max_lon, temp, np.nan)
temp = np.where(lat>=min_lat, temp, np.nan)
temp = np.where(lat<=max_lat, temp, np.nan)
temperature_avg = np.mean(temp[~np.isnan(temp)])

# RCP 4.5
# for i in range(len(time)):
#     precip = np.array(data_precip.variables['precipitation__map_rcp45_daily'][i,:])*1
#     precip = np.where(precip<=3000., precip, np.nan)
#     precip = np.where(long>=min_lon, precip, np.nan)
#     precip = np.where(long<=max_lon, precip, np.nan)
#     precip = np.where(lat>=min_lat, precip, np.nan)
#     precip = np.where(lat<=max_lat, precip, np.nan)
#     precipitation_avg = np.mean(precip[~np.isnan(precip)])

#     temp = np.array(data_temp.variables['air_temperature__map_rcp45_daily'][i,:])*1-273.15
#     temp = np.where(temp<=3000., temp, np.nan)
#     temp = np.where(long>=min_lon, temp, np.nan)
#     temp = np.where(long<=max_lon, temp, np.nan)
#     temp = np.where(lat>=min_lat, temp, np.nan)
#     temp = np.where(lat<=max_lat, temp, np.nan)
#     temperature_avg = np.mean(temp[~np.isnan(temp)])

# RCP 8.5
# for i in range(len(time)):
#     precip = np.array(data_precip.variables['precipitation__map_rcp85_daily'][i,:])*1
#     precip = np.where(precip<=3000., precip, np.nan)
#     precip = np.where(long>=min_lon, precip, np.nan)
#     precip = np.where(long<=max_lon, precip, np.nan)
#     precip = np.where(lat>=min_lat, precip, np.nan)
#     precip = np.where(lat<=max_lat, precip, np.nan)
#     precipitation_avg = np.mean(precip[~np.isnan(precip)])

#     temp = np.array(data_temp.variables['air_temperature__map_rcp85_daily'][i,:])*1-273.15
#     temp = np.where(temp<=3000., temp, np.nan)
#     temp = np.where(long>=min_lon, temp, np.nan)
#     temp = np.where(long<=max_lon, temp, np.nan)
#     temp = np.where(lat>=min_lat, temp, np.nan)
#     temp = np.where(lat<=max_lat, temp, np.nan)
#     temperature_avg = np.mean(temp[~np.isnan(temp)])

data_dict = {'Date': [date.strftime('%d/%m/%Y')], 'Month ID': [date.month],
             'Temp. (C)': [temperature_avg], 'Preci. (mm)': [precipitation_avg]}
xls_data=pd.concat([xls_data, pd.DataFrame.from_dict(data_dict)], ignore_index=True)
date += datetime.timedelta(days=1)

file_results = scenario + '_' + model + '_data.csv'
xls_data.to_csv(path_main_folder + '/' + file_results, index=False)

```

Appendix C

HBV Model - Python Script

This code is the function HBV that runs the HBV model.

Inputs:

ca = catchment area (km²)

n_{days} = number of days to be simulated
params = array with the 11 parameters of HBV in the following order [T_{thresh}, d, fc, beta, c, k0, l, k1, k2, kp, pwp]

air_{temp} = array with the timeseries (length n_{days}) of the daily-averaged air temperature (°C)

precip = array with the timeseries (length n_{days}) of the daily-accumulated precipitation (mm)

dpem = array with the daily potential evapotranspiration in each month (length 12 months) (mm/day)

Output:

qm = array with the timeseries (length n_{days}) of the simulated daily-averaged flow rate (m³/s)

```
import numpy as np

def HBV(ca, n_days, params, month, air_temp, prec, monthly, dpem):

    #Set parameters with reconizable names
    Tsnow_thresh = params[0] #threshold temperature for snow, generally equal to 0.0 (oC)
    d = params[1] #degree-day factor indicating the decrease of the water-content in
    #the snow cover caused by 1 oC above the freezing threshold in one day
    fc = params[2] #FC maximum soil storage capacity (mm)
    beta = params[3] #beta shape coefficient, which is a model parameter (-)
    c = params[4] #model parameter for the adjusted potential evapotranspiration (oC**-1)
    k0 = params[5] #K0 near surface flow storage coefficient (day**-1)
    l = params[6] #L threshold of the upper reservoir
    k1 = params[7] #K1 interflow storage coefficient (day**-1)
    k2 = params[8] #K2 groundwater storage coefficient (day**-1)
    kp = params[9] #Kperc percolation storage coefficient (day**-1)
    pwp = params[10] #PWP soil permanent wilting point, defined as the minimum amount
    #of water in the soil that the plant requires not to wilt (mm)

    #Initialize arrays for the simulation
    snow = np.zeros(air_temp.size) #SP Snow Pack (mm)
    liq_water = np.zeros(air_temp.size) #LW Liquid Water (mm)
    pe = np.zeros(air_temp.size) #PEa adjusted potential evapotranspiration (mm)
    soil = np.zeros(air_temp.size) #SM Soild Misture (mm)
    ea = np.zeros(air_temp.size) #Ea actual evapotranspiration (mm/day)
    dq = np.zeros(air_temp.size) #Peff effective precipitation (mm/day)
    s1 = np.zeros(air_temp.size) #SU storage upper reservoir (fast response runoff) (mm)
    s2 = np.zeros(air_temp.size) #SL storage lower reservoir (slow response runoff) (mm)
    q = np.zeros(air_temp.size) #Qtot total flow rate (mm/day)
    qm = np.zeros(air_temp.size) #Qtot total flow rate (m3/s)

    #Initiating the reservoirs
    snow[0] = 0. #SP Snow Pack (mm), the simulation should start 1st September,
    #ensuring that the SP = 0 at the beginning
    soil[0] = 100. #SM Soild Misture (mm)
    s1[0] = 2. #SU storage upper reservoir (fast response runoff) (mm)
    s2[0] = 200. #SL storage lower reservoir (slow response runoff) (mm)

    #Loop that runs through all days
```

```

for i_day in range(1,n_days):

if air_temp[i_day] <= Tsnow_thresh: #if the temperature is bellow or equal to the treshold
#Precip adds to the snow pack
snow[i_day] = snow[i_day-1] + prec[i_day]
#Too cold, no liquid water
liq_water[i_day] = 0.0
#Adjust potential ET base on difference between mean daily temp
#and long-term mean monthly temp
pe[i_day] = (1.+ c*(air_temp[i_day]-monthly[int(month[i_day])]))*dpem[int(month[i_day])])
#Check soil moisture and calculate actual evapotranspiration
if soil[i_day-1] >= pwp:
ea[i_day] = pe[i_day]
else:
#Reduced ET_actual by fraction of permanent wilting point
ea[i_day] = pe[i_day]*soil[i_day-1]/pwp

#Check soil moisture and calculate actual evapotranspiration
dq[i_day] = liq_water[i_day]*(soil[i_day-1]/fc)**beta

#Check soil moisture and calculate actual evapotranspiration
soil[i_day] = soil[i_day-1] + liq_water[i_day] - dq[i_day] - ea[i_day]

#Upper reservoir water level
s1[i_day] = s1[i_day-1] + dq[i_day] - max(0,s1[i_day-1]-1)*k0 - s1[i_day-1]*k1 - s1[i_day-1]*kp

#Lower reservoir water level
s2[i_day] = s2[i_day-1] + s1[i_day-1]*kp - s2[i_day-1]*k2

#Run-off is total from upper (fast/slow) and lower reservoirs
q[i_day] = max(0,s1[i_day]-1)*k0 + s1[i_day]*k1 + s2[i_day]*k2

#Resulting Q
qm[i_day] = (q[i_day]*ca*1000.)/(24.*3600.)

else: #if the temperature is above the treshold
#There is snow melting SP decreases or maintains a value 0
snow[i_day] = max(snow[i_day-1]-d*(air_temp[i_day]-Tsnow_thresh),0.)

#LW is precipitation plus snow melt
liq_water[i_day] = prec[i_day]+min(snow[i_day-1],d*(air_temp[i_day]-Tsnow_thresh))

#Adjust potential ET base on difference between mean daily temp
#and long-term mean monthly temp
pe[i_day] = (1.+ c*(air_temp[i_day]-monthly[int(month[i_day])]))*dpem[int(month[i_day])])

#Check soil moisture and calculate actual evapotranspiration
if soil[i_day-1] >= pwp:
ea[i_day] = pe[i_day]
else:
ea[i_day] = pe[i_day]*soil[i_day-1]/pwp

#Effective precip (portion that contributes to runoff)
if soil[i_day-1] > fc:
dq[i_day] = liq_water[i_day]
else:
dq[i_day] = liq_water[i_day]*((soil[i_day-1]/fc)**beta

#Soil moisture = previous days SM + liquid water - Direct Runoff - Actual ET
soil[i_day] = soil[i_day-1] + liq_water[i_day] - dq[i_day] - ea[i_day]

#Upper reservoir water level
s1[i_day] = s1[i_day-1] + dq[i_day] - max(0,s1[i_day-1]-1)*k0 - s1[i_day-1]*k1 - s1[i_day-1]*kp

#Lower reservoir water level
s2[i_day] = s2[i_day-1] + s1[i_day-1]*kp - s2[i_day-1]*k2

#Run-off is total from upper (fast/slow) and lower reservoirs
q[i_day] = max(0,s1[i_day]-1)*k0 + s1[i_day]*k1 + s2[i_day]*k2

#Resulting Q
qm[i_day] = (q[i_day]*ca*1000.)/(24.*3600.)

#End of simulation
return qm

```


Appendix D

HBV Model Calibration - Python Script

This code runs the calibration of the HBV model. The script saves the optimal results in .csv files for later use. The code prints the Nash Sutcliffe efficiency.

```
import numpy as np
import pandas as pd
from geneticalgorithm import geneticalgorithm as ga
from HBV_python import HBV

ca = 1780.66 #catchment area (km2)

#reading the daily potential evapotranspiration for each month
monthly, dpem = np.genfromtxt('inputMonthlyTempEvap2.txt', unpack=True, usecols=[0,2])

#reading the observed flow rate (NVE station)
data_NVE_station = pd.read_csv('Flakksvann.csv', sep = ";", decimal=',', header=1, usecols=[0,1])
data_NVE_station = data_NVE_station.rename(columns={data_NVE_station.columns[0]: "TimeStamp",
                                                    data_NVE_station.columns[1]: "Q_obs"})
data_NVE_station['TimeStamp'] = pd.to_datetime(data_NVE_station['TimeStamp'])
data_NVE_station = data_NVE_station.set_index(['TimeStamp']) #put the index as a timestamp

#reading the observed temperature and precipitation (area-averaged from MET stations)
data_MET_stations = pd.read_csv('inputPrecipTemp2.csv')
data_MET_stations = data_MET_stations.rename(columns={data_MET_stations.columns[0]: 'TimeStamp',
                                                    data_MET_stations.columns[2]: 'temp',
                                                    data_MET_stations.columns[3]: 'precip'})
data_MET_stations['TimeStamp'] = pd.to_datetime(data_MET_stations['TimeStamp'], format='%d/%m/%Y')
data_MET_stations = data_MET_stations.set_index(['TimeStamp']) #put the index as a timestamp

##### CALIBRATION #####
#creating the timeseries arrays for calibrating the HBV
start = '1981-09-01' #starting date of the calibration
end = '2000-08-31' #ending date of the calibration
month = data_MET_stations[start:end]['Month ID'].to_numpy(dtype=float)
temp = data_MET_stations[start:end]['temp'].to_numpy()
precip = data_MET_stations[start:end]['precip'].to_numpy()
q_obs = data_NVE_station[start:end].to_numpy().reshape(-1,)

#Inserts an extra NaN element in some arrays so that the index in HBV can start at 1
month = np.insert(month,0,np.nan)
temp = np.insert(temp,0,np.nan)
precip = np.insert(precip,0,np.nan)

#Objective function to be minimized by GA
def f(X):
    q_sim = HBV(ca, len(temp), X, month, temp, precip, monthly, dpem) #computes the flow rate by HBV
    q_sim = q_sim[1:] #removing the NaN in the first element
    # computes the Nash Sutcliffe
    nse = 1.0 - (np.sum((q_obs - q_sim)**2.))/(np.sum((q_obs - np.mean(q_obs))**2.))

    #constraint PWP<=FC introduced as a penalty
    pen = 0
    if X[10]>X[2]:
        pen = 2 + 1*(X[10]-X[2]) #penalty to verify the constraint PWP<=FC
    return 1-nse+pen #objective function to be minimized with penalty

#return -1.*nse #objective function (-nse) to be minimized, it corresponds
```

```

#to maximize nse

#ranges of the parameters Tsnow_tresh, d, fc, beta, c, k0, l, k1, k2, kp, pwp
varbound=np.array([[[-1,2],\
                    [1,5],\
                    [50,500],\
                    [1,4],\
                    [0.01,0.1],\
                    [0.1,1],\
                    [10,100],\
                    [0.1,1],\
                    [0.001,.1],\
                    [0.001,.1],\
                    [50,250]])

#parameters of the GA algorithm
algorithm_param = {'max_num_iteration': 200,\
                  'population_size':100,\
                  'mutation_probability':0.1,\
                  'elit_ratio': 0.01,\
                  'crossover_probability': 0.5,\
                  'parents_portion': 0.3,\
                  'crossover_type':'uniform',\
                  'max_iteration_without_improv':20}

model=ga(function=f,\
         dimension=11,\
         variable_type='real',\
         variable_boundaries=varbound,\
         algorithm_parameters=algorithm_param)

model.run()

param_opt = model.best_variable #get the optimal parameters
opt_nse = 1-model.best_function #get the maximum Nash Sutcliff
print('NSE training = ', opt_nse)
GA_report = 1-np.array(model.report) #get a list with all the Nash Sutcliff
#values troughout the GA iterations

#saving in csv files the optimal results that can be used afterwards
pd.DataFrame(param_opt).to_csv("optimal_parameters.csv", header=None, index=None)
pd.DataFrame(np.array(opt_nse).reshape(-1,)).to_csv("optimal_nse.csv", header=None, index=None)
pd.DataFrame(GA_report).to_csv("GA_report.csv", header=None, index=None)

```

Appendix E

HBV Model Validation - Python Script

This is the calibrated code that runs the validation. The code prints the Nash Sutcliffe efficiency and Pearson correlation coefficient.

```
import numpy as np
import pandas as pd
from geneticalgorithm import geneticalgorithm as ga
from HBV_python import HBV

ca = 1780.66 #catchment area (km2)

#reading the optimal parameters obtained in the calibration
param_opt = pd.read_csv('optimal_parameters.csv',header=None).to_numpy().reshape(-1,)

#reading the daily potential evapotranspiration for each month
monthly, dpem = np.genfromtxt('inputMonthlyTempEvap2.txt', unpack=True, usecols=[0,2])

#reading the observed flow rate (NVE station)
data_NVE_station = pd.read_csv('Flakksvann.csv',sep = ";",decimal=',',header=1,usecols=[0,1])
data_NVE_station = data_NVE_station.rename(columns={data_NVE_station.columns[0]: "TimeStamp",
                                                    data_NVE_station.columns[1]: "Q_obs"})
data_NVE_station['TimeStamp'] = pd.to_datetime(data_NVE_station['TimeStamp'])
data_NVE_station = data_NVE_station.set_index(['TimeStamp']) #put the index as a timestamp

#reading the observed temperature and precipitation (area-averaged from MET stations)
data_MET_stations = pd.read_csv('inputPrecipTemp2.csv')
data_MET_stations = data_MET_stations.rename(columns={data_MET_stations.columns[0]: 'TimeStamp',
                                                    data_MET_stations.columns[2]: 'temp',
                                                    data_MET_stations.columns[3]: 'precip'})
data_MET_stations['TimeStamp'] = pd.to_datetime(data_MET_stations['TimeStamp'],format='%d/%m/%Y')
data_MET_stations = data_MET_stations.set_index(['TimeStamp']) #put the index as a timestamp

##### VALIDATION #####
#creating the timeseries arrays for validation the HBV (joining two periods)
start1 = '1972-09-01' #start date of 1st period of validation
end1 = '1981-08-31' #end date of 1st period of validation
start2 = '2000-09-01' #start date of 2nd period of validation
end2 = '2004-08-31' #end date of 2nd period of validation
month = np.concatenate((data_MET_stations[start1:end1]['Month ID'].to_numpy(dtype=float),
                        data_MET_stations[start2:end2]['Month ID'].to_numpy(dtype=float)))
temp = np.concatenate((data_MET_stations[start1:end1]['temp'].to_numpy(),
                        data_MET_stations[start2:end2]['temp'].to_numpy()))
precip = np.concatenate((data_MET_stations[start1:end1]['precip'].to_numpy(),
                          data_MET_stations[start2:end2]['precip'].to_numpy()))
q_obs = np.concatenate((data_NVE_station[start1:end1].to_numpy().reshape(-1),
                          data_NVE_station[start2:end2].to_numpy().reshape(-1)))

#Inserts an extra NaN element in some arrays so that the index in HBV can start at 1
month = np.insert(month,0,np.nan)
temp = np.insert(temp,0,np.nan)
precip = np.insert(precip,0,np.nan)

#computes the flow rate by HBV
q_sim = HBV(ca, len(temp), param_opt, month, temp, precip, monthly, dpem)
q_sim = q_sim[1:] #removing the NaN in the first element
# computes the Nash Sutcliffe
nse = 1.0 - (np.sum((q_obs - q_sim)**2.))/(np.sum((q_obs - np.mean(q_obs))**2.))
print('NSE validation = ', nse)

r = np.corrcoef(q_obs, q_sim)
print(r[1,0])
```

Appendix F

HBV Model Simulated Discharge - Python Script

These scripts must be run for each individual model with the associated time period or scenario. The output is an array with the timeseries of the simulated daily-averaged flow rate.

The script for the historical period (1971-2005):

```
import numpy as np
import pandas as pd
from geneticalgorithm import geneticalgorithm as ga
from HBV_python import HBV

ca = 1780.66 #catchment area (km2)

#reading the optimal parameters obtained in the calibration
param_opt = pd.read_csv('optimal_parameters.csv',header=None).to_numpy().reshape(-1,)

#reading the daily potential evapotranspiration for each month
monthly, dpem = np.genfromtxt('inputMonthlyTempEvap2.txt', unpack=True, usecols=[0,2])

#reading the observed temperature and precipitation
data_MET_stations = pd.read_csv('') #Change the climate model here for each run
data_MET_stations = data_MET_stations.rename(columns={data_MET_stations.columns[0]: 'TimeStamp',
                                                    data_MET_stations.columns[2]: 'temp',
                                                    data_MET_stations.columns[3]: 'precip'})
data_MET_stations['TimeStamp'] = pd.to_datetime(data_MET_stations['TimeStamp'],format='%d/%m/%Y')
data_MET_stations = data_MET_stations.set_index(['TimeStamp']) #put the index as a timestamp

#creating the timeseries arrays
start1 = '1971-01-01' #start date of 1st period of validation
end1 = '2005-12-31' #end date of 1st period of validation
month = data_MET_stations[start1:end1]['Month ID'].to_numpy(dtype=float)
temp = data_MET_stations[start1:end1]['temp'].to_numpy()
precip = data_MET_stations[start1:end1]['precip'].to_numpy()

#computes the flow rate by HBV
q_sim = HBV(ca, len(temp), param_opt, month, temp, precip, monthly, dpem)
q_sim = q_sim[1:] #removing the NaN in the first element

np.savetxt('q_sim.csv', q_sim, delimiter=',', fmt='%.6f')
```

The script for climate scenario RCP4.5:

```
import numpy as np
import pandas as pd
from geneticalgorithm import geneticalgorithm as ga
from HBV_python import HBV

ca = 1780.66 #catchment area (km2)

#reading the optimal parameters obtained in the calibration
```

```

param_opt = pd.read_csv('optimal_parameters.csv',header=None).to_numpy().reshape(-1,)

#reading the daily potential evapotranspiration for each month
monthly, dpem = np.genfromtxt('inputMonthlyTempEva_rcp4.5.txt', unpack=True, usecols=[0,2])

#reading the observed temperature and precipitation
data_MET_stations = pd.read_csv('') #Change the climate model here for each run
data_MET_stations = data_MET_stations.rename(columns={data_MET_stations.columns[0]: 'TimeStamp',
                                                    data_MET_stations.columns[2]: 'temp',
                                                    data_MET_stations.columns[3]: 'precip'})
data_MET_stations['TimeStamp'] = pd.to_datetime(data_MET_stations['TimeStamp'],format='%d/%m/%Y')
data_MET_stations = data_MET_stations.set_index(['TimeStamp']) #put the index as a timestamp

#creating the timeseries arrays
start1 = '2006-01-01' #start date of 1st period of validation
end1 = '2100-12-31' #end date of 1st period of validation
month = data_MET_stations[start1:end1]['Month ID'].to_numpy(dtype=float)
temp = data_MET_stations[start1:end1]['temp'].to_numpy()
precip = data_MET_stations[start1:end1]['precip'].to_numpy()

#computes the flow rate by HBV
q_sim = HBV(ca, len(temp), param_opt, month, temp, precip, monthly, dpem)
q_sim = q_sim[1:] #removing the NaN in the first element

np.savetxt('q_sim.csv', q_sim, delimiter=',', fmt='%.6f')

```

The script for climate scenario RCP8.5:

```

import numpy as np
import pandas as pd
from geneticalgorithm import geneticalgorithm as ga
from HBV_python import HBV

ca = 1780.66 #catchment area (km2)

#reading the optimal parameters obtained in the calibration
param_opt = pd.read_csv('optimal_parameters.csv',header=None).to_numpy().reshape(-1,)

#reading the daily potential evapotranspiration for each month
monthly, dpem = np.genfromtxt('inputMonthlyTempEva_rcp8.5.txt', unpack=True, usecols=[0,2])

#reading the observed temperature and precipitation
data_MET_stations = pd.read_csv('') #Change the climate model here for each run
data_MET_stations = data_MET_stations.rename(columns={data_MET_stations.columns[0]: 'TimeStamp',
                                                    data_MET_stations.columns[2]: 'temp',
                                                    data_MET_stations.columns[3]: 'precip'})
data_MET_stations['TimeStamp'] = pd.to_datetime(data_MET_stations['TimeStamp'],format='%d/%m/%Y')
data_MET_stations = data_MET_stations.set_index(['TimeStamp']) #put the index as a timestamp

#creating the timeseries arrays
start1 = '2006-01-01' #start date of 1st period of validation
end1 = '2100-12-31' #end date of 1st period of validation
month = data_MET_stations[start1:end1]['Month ID'].to_numpy(dtype=float)
temp = data_MET_stations[start1:end1]['temp'].to_numpy()
precip = data_MET_stations[start1:end1]['precip'].to_numpy()

#computes the flow rate by HBV
q_sim = HBV(ca, len(temp), param_opt, month, temp, precip, monthly, dpem)
q_sim = q_sim[1:] #removing the NaN in the first element

np.savetxt('q_sim.csv', q_sim, delimiter=',', fmt='%.6f')

```

Bibliography

- [1] Climate.gov. “Climate change: Global temperature.” (), [Online]. Available: <https://www.climate.gov/news-features/understanding-climate/climate-change-global-temperature>. (accessed: 04.05.2023).
- [2] U. Sydnes. “Slår alarm: – aldri sett innsjøen så uttørket.” (), [Online]. Available: <https://www.tv2.no/nyheter/utenriks/slar-alarm-aldri-sett-innsjoen-sa-uttorket/15530426/>. (accessed: 05.05.2023).
- [3] NationalGeographic. “Day zero: Where next?” (), [Online]. Available: <https://www.nationalgeographic.com/science/article/partner-content-south-africa-danger-of-running-out-of-water>. (accessed: 14.05.2023).
- [4] USGS. “Low-lying areas of tropical pacific islands.” (), [Online]. Available: <https://www.usgs.gov/centers/pcmssc/science/low-lying-areas-tropical-pacific-islands>. (accessed: 14.05.2023).
- [5] EUCommission. “Eu supporting belgium with flood response.” (), [Online]. Available: https://ec.europa.eu/commission/presscorner/detail/en/IP_21_37211. (accessed: 14.05.2023).
- [6] NYTimes. “A quarter of bangladesh is flooded. millions have lost everything.” (), [Online]. Available: <https://www.nytimes.com/2020/07/30/climate/bangladesh-floods.html>. (accessed: 14.05.2023).
- [7] NationalGeographic. “As ice melts, the inuit strive to keep their culture alive.” (), [Online]. Available: <https://www.nationalgeographic.com/culture/article/inuit-share-traditional-knowledge-to-survive-melting-ice-feature>. (accessed: 14.05.2023).
- [8] FN-sambandet. “Parisavtalen.” (), [Online]. Available: <https://www.fn.no/om-fn/avtaler/miljoe-og-klima/parisavtalen>. (accessed: 03.05.2023).
- [9] UN. “The 17 goals.” (), [Online]. Available: <https://sdgs.un.org/goals/goal7>. (accessed: 03.05.2023).
- [10] Statkraft. “Vannkraft.” (), [Online]. Available: <https://www.statkraft.no/var-virksomhet/vannkraft/>. (accessed: 03.05.2023).
- [11] NVE. “Kraftproduksjon.” (), [Online]. Available: www.nve.no/energi/energisystem/kraftproduksjon/. (accessed: 03.05.2023).
- [12] ÅEnergi. “Å energi øker tempoet i fornybarsatsingen.” (), [Online]. Available: <https://www.aenergi.no/no/nyheter/a-energi-oket-tempoet-i-fornybarsatsingen>. (accessed: 15.05.2023).
- [13] S. Turner and N. Voisin, “Simulation of hydropower at subcontinental to global scales: A state-of-the-art review,” *Environ. Res. Lett*, 2022.
- [14] O. Hoes, L. Meijer, R. van der Ent, and N. van de Giesen, “Systematic high-resolution assessment of global hydropower potential,” *PLoS ONE*, 2017.
- [15] P. Maher and N. Smith. “Pico hydro for village power.” (), [Online]. Available: https://energypedia.info/images/9/92/Ph_manual_s.pdf. (accessed: 20.04.2023).
- [16] Unknown. “Hydraulic turbines and hydroelectric power plants.” (), [Online]. Available: https://www.fer.unizg.hr/_download/repository/Hydraulic_turbines_HPP.pdf. (accessed: 20.04.2023).

- [17] GITTA. “Thiessen polygon.” (), [Online]. Available: http://www.gitta.info/Accessibilit/en/html/UncProxAnaly_learningObject4.html. (accessed: 15.04.2023).
- [18] J. Leal, “Hydrology, pp presentation,” Unpublished.
- [19] ArcGISpro. “Create thiessen polygons (analysis).” (), [Online]. Available: <https://pro.arcgis.com/en/pro-app/latest/tool-reference/analysis/create-thiessen-polygons.htm>. (accessed: 15.04.2023).
- [20] L. Ávila, R. Silveira, A. Campos, *et al.*, “Comparative evaluation of five hydrological models in a large-scale and tropical river basin.,” *Water*, vol. 14,3013, 2022.
- [21] Z. Liu, Y. Wang, Z. Xu, and Q. Duan, “Conceptual hydrological models,” in *Handbook of Hydrometeorological Ensemble Forecasting*. Springer Berlin Heidelberg, 2017, pp. 1–23.
- [22] G. Devia, B. Ganasri, and G. Dwarakish, “A review on hydrological models,” *Aquatic Procedia*, 2015.
- [23] Z. Islam, “A review on physically based hydrologic modeling,” *ResearchGate*, 2011.
- [24] A. Aghakouchak and E. Habib, “Application of a conceptual hydrologic model in teaching hydrologic processes,” *Int. J. Engng Ed.*, 2010.
- [25] T. Stocker, D. Qin, G. Plattner, *et al.*, “Climate change 2013: The physical science basis. contribution of working group i to the fifth assessment report of the intergovernmental panel on climate change,” *IPCC*, 2013.
- [26] C. Bjørnæs. “A guide to representative concentration pathways.” (), [Online]. Available: <https://cicero.oslo.no/en/articles/a-guide-to-representative-concentration-pathways>. (accessed: 19.04.2023).
- [27] H. Hisdal, E. Holmqvist, J. Jónsdóttir, *et al.*, “Has streamflow changed in the nordic countries?” *NVE*, 2010.
- [28] D. Wilson, H. Hisdal, and D. Lawrence, “Has streamflow changed in the nordic countries? – recent trends and comparisons to hydrological projections,” *Journal of Hydrology*, vol. 394 (3–4): 334–346. 2010.
- [29] E. Holmqvist, “Norges vannbalanse i twh basert på hbv-modeller,” *NVE*, vol. 35 pp, 2014.
- [30] L. A. Roald, S. Beldring, T. E. Skaugen, E. J. Førland, and R. Benestad, “Climate change impacts on streamflow in norway,” *NVE*, vol. 73 pp, 2006.
- [31] I. Hanssen-Bauer, E. Førland, I. Haddeland, *et al.*, “Klima i norge 2100,” *Miljødirektoratet.no*, vol. 204 pp, 2015.
- [32] NCCS. “Klimaprofil agder.” (), [Online]. Available: <https://klimaservicesenter.no/kss/klimaprofiler/agder>. (accessed: 11.04.2023).
- [33] V. Koestler, A. Østenby, C. Birkeland, F. Arnesen, and I. Haddeland, “Vannkraftverkene i norge får mer tilsig,” *NVE*, 2019.
- [34] H. Wang, W. Xiao, Y. Wang, *et al.*, “Assessment of the impact of climate change on hydropower potential in the nanliujiang river basin of china,” *Energy*, 2018.
- [35] W. Dilnesa, “Gis and hydrological model based hydropower potential assessments of temcha watershed,” *IJEGEO*, 2022.
- [36] R. Nonki, A. Lenouo, C. Tchawoua, C. Lennard, and E. Amoussou, “Impact of climate change on hydropower potential of the lagdo dam, benue river basin, northern cameroon,” *IAHS*, 2021.
- [37] S. Bhattarai, Y. Zhou, N. Shakya, and C. Zhao, “Hydrological modelling and climate change impact assessment using hbv light model: A case study of narayani river basin, nepal,” *nep-tjournal*, 2017.
- [38] D. Lawrence, I. Haddeland, and E. Langsholt, “Calibration of hbv hydrological models using pest parameter estimation,” *ResearchGate*, 2009.
- [39] NVE. “Hbv-modellen.” (), [Online]. Available: <https://www.nve.no/vann-og-vassdrag/vannets-kretsloep/analysemetoder-og-modeller/hbv-modellen/>. (accessed: 02.05.2023).

- [40] UZH. “Hbv-light model.” (), [Online]. Available: <https://www.geo.uzh.ch/en/units/h2k/Services/HBV-Model.html>. (accessed: 02.05.2023).
- [41] A. AghaKouchak, N. Nakhjiri, and E. Habib, “An educational model for ensemble streamflow simulation and uncertainty analysis,” *Hydrol. Earth Syst. Sci.*, 2012.
- [42] Vannportalen. “Om agder vannregion.” (), [Online]. Available: www.vannportalen.no/vannregioner/agder/om-vannregion-agder2/. (accessed: 17.04.2023).
- [43] W. Wong, I. Haddeland, D. Lawrence, and S. Beldring, “Gridded 1 x 1 km climate and hydrological projections for norway,” *NVE*, 2016.
- [44] D. Jacob, J. Petersen, B. Eggert, and et al., “Euro-cordex: New high-resolution climate change projections for european impact research,” *Reg Environ Change*, 2014.
- [45] MET, NVE, NORCE, and BCCR. “Seklima - observasjoner og værstatistikk.” (), [Online]. Available: <https://seklima.met.no/observations>. (accessed: 16.03.2023).
- [46] NVE. “Sildre.” (), [Online]. Available: <https://sildre.nve.no/map?x=380400&y=7228000&zoom=4>. (accessed: 16.03.2023).
- [47] ClimateEngine. “Climateengine.” (), [Online]. Available: <https://app.climateengine.com/climateEngine>. (accessed: 16.03.2023).
- [48] A. Aghakouchak. “Introduction to hydrologic modeling: A hands-on practice by amir aghakouchak.” (), [Online]. Available: <https://www.youtube.com/watch?v=SYqKCu81AVM>. (accessed: 23.03.2023).
- [49] D. Moriasi, J. Arnold, M. van Liew, R. Bingner, R. Harmel, and T. Veith, “Model evaluation guidelines for systematic quantification of accuracy in watershed simulations,” *American Society of Agricultural and Biological Engineers*, 2007.
- [50] M. Selvanathan, N. Jayabalan, G. Saini, M. Supramaniam, and N. Hussain, “Employee productivity in malaysian private higher educational institutions.,” *PalArch’s Journal of Archaeology of Egypt/ Egyptology*, vol. 17, pp. 66–79, 2020. DOI: 10.48080/jae.v17i3.50.